AEDC-TDR-64-47

AN EXPERIMENTAL STUDY OF DIFFUSERS IN AN OPEN-JET, LOW-DENSITY, HYPERSONIC WIND TUNNEL

By

David E. Boylan
von Kármán Gas Dynamics Facility
ARO, Inc.

TECHNICAL DOCUMENTARY REPORT NO. AEDC-TDR-64-47

April 1964

Program Element 62405334/8950, Task 895004

(Prepared under Contract No. AF 40(600)-1000 by ARO, Inc., contract operator of AEDC, Arnold Air Force Station, Tenn.)

ARNOLD ENGINEERING DEVELOPMENT CENTER

AIR FORCE SYSTEMS COMMAND

UNITED STATES AIR FORCE

PROPERTY OF U. S. AIR FORCE

NOTICES

Qualified requesters may obtain copies of this report from DDC, Cameron Station, Alexandria, Va. Orders will be expedited if placed through the librarian or other staff member designated to request and receive documents from DDC.

When Government drawings, specifications or other data are used for any purpose other than in connection with a definitely related Government procurement operation, the United States Government thereby incurs no responsibility nor any obligation whatsoever; and the fact that the Government may have formulated, furnished, or in any way supplied the said drawings, specifications, or other data, is not to be regarded by implication or otherwise as in any manner licensing the holder or any other person or corporation, or conveying any rights or permission to manufacture, use, or sell any patented invention that may in any way be related thereto.

AEDC-TDR-64-47

AN EXPERIMENTAL STUDY OF DIFFUSERS IN AN OPEN-JET, LOW-DENSITY, HYPERSONIC WIND TUNNEL

By

David E. Boylan

von Kármán Gas Dynamics Facility

ARO, Inc.

a subsidiary of Sverdrup and Parcel, Inc.

April 1964

ARO Project No. VL2407

AF - AEDC
Arnold AFS Tenn

FOREWORD

The author wishes to acknowledge the assistance of A. B. Bailey who did the initial design of the diffusers and J. Leith Potter who initiated the study, provided many helpful suggestions during the course of the investigations, and assisted in the analysis of the results.

ABSTRACT

An experimental investigation of supersonic diffuser performance in a flow regime in which viscous and compressibility influences are equally important was conducted. The investigation involved Mach numbers from 6 to 16.5. It is shown that, although diffuser recovery compared to higher density regimes is small, using the proper diffuser allowed the required wind tunnel exhaust pressure to be up to 35 times the pressure existing in the test chamber. While this may not seem exceptional at first glance, it is important to note that this was achieved in conjunction with Reynolds numbers on the order of 10^{-3} below those typical of tunnels yielding higher recoveries.

For a given test condition, it was found that diffuser throat area was the dominant parameter in determining the increase in nozzle pressure ratio resulting from diffuser pressure recovery, with diffuser throat length becoming increasingly important with decreasing viscous effects, i.e., at higher Reynolds numbers. The change in pressure recovery created by the addition of a model in the stream also was investigated for a range of flow and diffuser conditions. A complex flow model which sometimes includes supersonic flow throughout the length of the diffuser, oblique shock interaction with very thick boundary layers, and reverse flow near the wall of some diffuser inlets was found to exist.

PUBLICATION REVIEW

This report has been reviewed and publication is approved.

Larry R. Walter
1st Lt, USAF
DCS/Research

Donald R. Eastman, Jr.
DCS/Research

CONTENTS

		Page
	ABSTRACT	v
	NOMENCLATURE	xi
1.0	INTRODUCTION	1
2.0	APPARATUS	
	2.1 The Wind Tunnel	1
	2.2 Pressure Instrumentation System	2
	2.3 Diffuser Components	2
	2.4 Blockage Models	4
3.0	EXPERIMENTAL PROCEDURE	
	3.1 Test Conditions	4
	3.2 Pressure Data and Procedure	5
4.0	CAPACITY OF TUNNEL PUMPING SYSTEM	6
5.0	DISCUSSION OF DIFFUSER THEORY AND EXPERIENCE	
	5.1 Nature of Test Chamber Pressure Control	8
6.0	EXPERIMENTAL RESULTS WITH NO BLOCKAGE	
	6.1 Effects of Variables Studied	10
7.0	NATURE OF THE FLOW IN THE DIFFUSER	13
8.0	ANALYSIS OF THE EXPERIMENTAL RESULTS	14
	8.1 Pressure Ratios Available in Tunnel L	15
	8.2 Free Jet Length and Diffuser Inlet Angle	15
	8.3 Area Ratio Effects	16
	8.4 Diffuser Throat Length	17
9.0	PRESSURE RECOVERY	17
10.0	EXPERIMENTAL RESULTS OF BLOCKAGE TESTS	19
11.0	CONCLUDING REMARKS	21
	REFERENCES	22

TABLES

1. Test Conditions 25
2. Optimum Diffuser Performance 26

ILLUSTRATIONS

Figure

1. Schematic of Tunnel L 27
2. Photograph of Tunnel L from the Operator's Side 28

Figure		Page
3.	Diffuser Components	29
4.	Blockage Models	30
5.	Diffuser with Wall Static-Pressure Tubes Installed in Tunnel	31
6.	Tunnel Ejector Capacity	32
7.	Effect of Free-Jet Length	33
8.	Effect of Diffuser Throat Area	34
9.	Effect of Inlet Section Angle	35
10.	Effect of Diffuser Components	
	a. Diffuser Throat Area at or Near Optimum (Flow Condition 1)	36
	b. Diffuser Throat Area Not Near Optimum (Flow Condition 1)	37
	c. Diffuser Throat Area Near Optimum (Flow Condition 2)	38
	d. Diffuser with Optimum Inlet and Long Throat (Flow Condition 2)	39
	e. Diffuser with Optimum Inlet and Long Throat (Flow Condition 3)	40
	f. Diffuser with Optimum Inlet and Long Throat (Flow Condition 4)	41
11.	Nozzle Shock System Revealed by Natural Flow Visualization	
	a. Flow Condition 3, $p_T \approx 110\ \mu$Hg, $p_\infty \approx 220\ \mu$Hg	42
	b. Flow Condition 3, $p_T \approx 550\ \mu$Hg, $p_\infty \approx 220\ \mu$Hg	43
12.	Centerline and Wall Pressure Surveys	44
13.	Typical Lateral Pressure Surveys	45
14.	Flow Field Near Inlet Plane as Revealed by Yarn Tufts	46
15.	Typical Flow Model	47
16.	Pressure Ratios Available	48
17.	Effect of Diffuser Area Ratio on Test Chamber Pressure	49
18.	Diffuser Efficiency as a Function of Reynolds Number	50

Figure		Page
19.	Typical Blockage Results	51
20.	Effect of Model Size and Shape on Tunnel Blockage	54
21.	Effect of Sting Length on Tunnel Blockage	57
22.	Effect of Model Blockage with Diffuser Throat Diameter as a Parameter	58

NOMENCLATURE

A	Area
D	Diameter
FJL	Free-jet length
H	Enthalpy
K	Total pressure ratio
L	Length
M	Mach number
m	Tunnel mass-flow rate
p	Pressure
p_o'	Stagnation pressure downstream of a normal shock
p_o/p_6	Tunnel pressure ratio
p_o/p_T	Nozzle pressure ratio
R	Gas constant
Re	Reynolds number
r	Radius
S	Entropy
T	Temperature
v	Velocity
x	Distance from nozzle exit plane, negative upstream
y	Distance from nozzle centerline, negative below
α_i	Diffuser inlet angle
γ	Ratio of specific heats
δ	Boundary-layer thickness
η_D	Diffuser efficiency defined by Eq. (3)
θ_n	Nozzle exit wall angle
λ	Mean free path
μ	Microns

SUBSCRIPTS

1	Nozzle exit plane
2	Diffuser inlet plane
3	Diffuser throat entrance plane
4	Diffuser throat exit plane
5	Diffuser exit plane
6	Plane just upstream of first ejector
e	Divergent section of diffuser
e.c.	Expansion core - related to A/A^* at M_1
i	Contraction section of diffuser
m	Point of maximum expansion of flow
NS	Normal shock
n	Aerodynamic nozzle
o	Stagnation conditions
s	Diffuser insert
T	Test chamber
t	Throat section of diffuser
w	Diffuser wall
∞	Free-stream conditions in inviscid core at nominal test section

SUPERSCRIPT

*	Sonic point

1.0 INTRODUCTION

One of the critical design problems in simulating flight at high altitudes and Mach numbers in a wind tunnel arises because of the large pressure ratios required. The problem becomes even more critical if a continuous-flow facility is desired because of the expense of pumping systems to handle the required mass-flow rate at low pressures.

Supersonic diffusers have been used in various facilities for some time to provide enough pressure recovery to bridge the gap between pressure ratios provided by the pumping system and those needed to provide suitable shock-free flow in the test region. However, available data for hypersonic, very-low-density flow are essentially nonexistent except for the brief study reported in Ref. 1. The Gas Dynamic Wind Tunnel, Hypersonic L of the von Kármán Gas Dynamics Facility (VKF), Arnold Engineering Development Center (AEDC), Air Force Systems Command (AFSC), has been used to extend the study described in Ref. 1. This report contains data and analysis of diffuser performance for a range of test conditions in Tunnel L.

2.0 APPARATUS

2.1 THE WIND TUNNEL

Tunnel L is a continuous, arc-heated, ejector-pumped design. Figure 1 is a schematic of the nozzle, test chamber, and diffuser area to the first ejector. Also shown schematically is the pressure instrumentation system which is placed inside the test chamber. Figure 2 is a photograph of the tunnel showing the arc heater and control panel. The major components are (1) a d-c arc-heater of the constricted, nonrotated arc and non-swirl gas injection type with a 40-kw power supply, (2) a settling section of variable length but normally about 6 in. long; (3) aerodynamic nozzles of varying design, (4) a test chamber of 48-in. diameter surrounding the test section and containing instrumentation and probe carrier, (5) an interchangeable diffuser, (6) a heat exchanger, (7) an air-ejector of two stages, and (8) the VKF vacuum pumping system. All critical components of the tunnel are protected by back-side water

---

Manuscript received February 1964.

cooling. The two-stage ejector system is driven by air instead of steam because of the ready availability of the former in the present case. This tunnel has proved highly satisfactory, always yielding data of excellent repeatability. The working gas normally is nitrogen or argon, although other gases may by used. An earlier description of the tunnel is given in Ref. 1.

2.2 PRESSURE INSTRUMENTATION SYSTEM

Low-density wind tunnel pressure instrumentation presents several problems which must be overcome before accurate measurements can be made. One great advantage of the present facility is the long flow duration which makes it possible (in most cases) to "outwait" the lag time of the measuring system.

The major components of the pressure measuring system are

1. pressure transducers and associated readout system,
2. scanner valves,
3. reference and calibration pressure systems with associated valves and tubing,
4. micromanometer and McLeod gage for calibration of transducers and measurement of reference pressure.

A description of these components is given in Ref. 2. Calibrations for a given transducer almost always remain constant for an extended period of time. However, as a check, calibrations were obtained many times throughout the test period, and any small deviations were taken into account.

2.3 DIFFUSER COMPONENTS

It was not considered practical to construct a diffuser of variable geometry because of the desire to investigate a wide variety of diffuser and flow conditions. From a general knowledge of open-jet diffuser design and from the limited experience obtained in Tunnel L on diffuser performance, the diffuser components shown in Fig. 3 were designed and built.

The components are capable of being interchanged with each other to a certain extent and are all provided with "O"-ring seals to prevent

leakage. The diffuser is placed inside a 10-in.-diam pipe which in turn is telescoped into the downstream tunnel ducting. This 10-in. pipe may be moved upstream or downstream, thereby changing the free-jet length of the flow, which is defined as the distance from the nozzle exit to the diffuser inlet. Backflow around the 10-in. pipe is prevented by an "O"-ring seal placed as shown in Fig. 1. Pins installed downstream of the test chamber can be moved from outside the tunnel to align the diffuser with the tunnel centerline.

Since the aerodynamic nozzles of Tunnel L are axisymmetric, the diffusers were also constructed in this manner rather than the two-dimensional configuration often seen in diffuser design. In Fig. 3, each diffuser component is given an identifying number or letter. A complete diffuser is composed of up to four components, the entrance, throat components, and exit. In the text and figures, a particular diffuser is identified by a code such as 30-10+20-40. These are the drawing numbers for the various components and are explained by reference to tables in Fig. 3. For example, 30-10+20-40 indicates, from Fig. 3, a 6-in.-diam throat, 2.59-in.-long inlet section of 30 deg half-angle, 3-in.- and 6-in.-long throat sections for a total throat length of 9 in., and a 5.6-in.-long divergent final section of 15 deg half-angle. The first number always corresponds to the entrance section (Fig. 3, Table 1), the middle two numbers correspond to the throat components (Fig. 3, Table 2), and the last corresponds to the exit component (Fig. 3, Table 3). A zero indicates the absence of a particular section which would ordinarily be in place. Thus, 30-0+0-0 indicates that only the entrance section of the diffuser was being tested.

Throat components 7C, 7D, 7E, 7F, 7G, and 25 (Fig. 3, Table 2) were constructed to determine the effect resulting from a throat length considerably longer than the 9-in. maximum available from the other components. Throat component 25 was tested with inlet section 180M which was modified from component 180 to receive the larger diameter of the throat. This diffuser is identified as 180M-0+25-0 in order to be consistent with other nomenclature.

Two inserts to fit into the 30-deg inlets were constructed so that a further reduction in throat size could be obtained. These inserts were of thin sheet metal and could be attached to the inlet wall by high-temperature adhesive tape.

Table 1 gives nozzle dimensions and the several flow parameters for each of the flow conditions run during the present investigation. Included are flow properties at several stations on the nozzle centerline in the normal test region, indicating the axial-flow gradients existing. Also included are values of the expansion core radius at the nozzle exit determined from the calibrated Mach number and the experimentally determined boundary-layer thickness on the nozzle wall at the exit plane.

For one-dimensional, inviscid, fluid flow in an overexpanded, axisymmetric nozzle, a conical shock system may be assumed to originate near the nozzle exit lip and focus on the nozzle centerline at some point downstream of the exit. The point of intersection is determined by pressure ratio and nozzle exit Mach number. Effects created by very thick boundary layers and multiple or fan-type shocks make the analytic prediction of the position of the trailing shock difficult, if not impossible, in Tunnel L.

The volume upstream of the centerline shock intersection, within the inviscid core, is defined as the nozzle test section. Both the length and diameter of this volume are variable. The diameter is a function of the nozzle geometry and the flow conditions which determine the boundary-layer thickness. The length is primarily a function of nozzle geometry, the pressure ratio $p_T/p_{\infty 1}$, and Mach number for a given flow condition.

As the test chamber pressure is reduced, p_T will approach p_∞. As this happens the flow will expand to a higher Mach number and lower p_∞ until equilibrium between p_T and p_∞ is reached. However, as $p_T \rightarrow p_\infty$, the shock strength will be reduced, with the limiting case of no exit shock when $p_T = p_\infty$. A further reduction in p_T will result in the nozzle operating underexpanded. The test chamber pressure at which the nozzle shock system travels upstream of the desired test region is defined as the limit at which the tunnel flow breaks down.

3.2 PRESSURE DATA AND PROCEDURE

Flow calibrations determined the impact-pressure gradients in the free stream and in the boundary layer in the vicinity of the nozzle exit. A small 0.125-in. O. D. impact probe was used to measure pressures upstream of the diffuser inlet beginning at a point 1.0 in. from the diffuser inlet plane. This probe was used to obtain both centerline and lateral surveys across the diffuser inlet. The probe could be completely removed from the flow field so that diffuser performance could be studied with a clear jet. Further instrumentation of the diffusers

with $L_t \leq 9$ in. was made by placing a 0.250-in. O. D. probe on the centerline at the diffuser exit. This probe could be placed facing upstream or downstream to record either total or base pressures in this plane. For practical reasons, the pressure line from this probe had to be routed upstream along the inner wall of the diffuser to reach the transducer. Each diffuser was run with and without this exit probe to study any effect the probe had on diffuser performance. Data which were affected by the presence of the probe have been omitted, and a discussion of the blockage effect is included in Section 10.0.

The diffuser configurations with $L_t > 9$ in. were instrumented with a centerline impact probe and wall static probe at the exit to determine the Mach number existing at this station.

After the initial series of tests was completed, diffuser number 26-6+16-36 was instrumented to measure wall static pressure by placing a series of open-ended 0.125-in. O. D. tubes (facing downstream) along the diffuser walls at various stations. Figure 5 shows the diffuser installed in the tunnel with several of these pressure tubes connected to the transducers.

A probe placed at station 6 (see Fig. 1) could be rotated to read either total or static pressure. This measurement was made with a precision micromanometer similar to the one used in the calibration system. Impact pressures within the diffuser were measured with a series of 0.125-in. O. D. probes constructed in a "trombone" manner so that they could be inserted into the inlet and throat areas of the diffuser and moved by the probe carrier located upstream of the diffuser as shown in Fig. 1. The re-entrant or return portions of these trombone-shaped probes lay near the diffuser wall where dynamic pressures were very low and the probes had no apparent effect on the upstream flow.

4.0 CAPACITY OF TUNNEL PUMPING SYSTEM

The pumping system of the tunnel consists of a two-stage air-ejector system and the VKF vacuum system. The VKF vacuum system consists of a 200,000-cu-ft spherical vacuum reservoir and large, mechanical, vacuum pumps. The reservoir is normally kept at a pressure on the order of 3000 to 8000 μHg by the pumps while the tunnel is in operation. The two-stage air ejector further reduces the tunnel presure to approximately 10-30 μHg when no flow is being introduced into the tunnel, and this performance is independent of sphere pressure when the latter is below approximately 8000 μHg. Because of

the large capacity of the sphere and the relatively low mass-flow rates used in Tunnel L, operation is continuous, with a run duration of hours being possible.

In order to determine the blank-off pressure and to establish the performance capabilities of the ejector system, an experiment was conducted. The aerodynamic nozzle was sealed at the settling chamber so that no flow could enter the nozzle. A measured amount of the test gas was allowed to flow into the test chamber from a port located in the test chamber at a right angle to the axis of the diffuser. At each leak rate, a minimum value of p_T was reached by the proper adjustment of the ejector controls. Since the rate of flow entering the diffuser was small and, so-to-speak, non-directed, the jet-pump action of the flow entering the diffuser should have had little effect on the minimum p_T obtainable, and the results should be an indication of the capacity of the ejector system with minimum diffuser action. Figure 6 shows the results of the experiment and reveals that the blank-off pressure was 25 μHg under the conditions existing at the time of the test.

How much the blank-off pressure is influenced by leakage and outgassing is hard to predict. Experience has shown that if the tunnel is allowed to outgas for several hours, the minimum p_T obtainable with no flow is reduced by as much as 5 μHg.

The validity of the assumption that the diffuser produced no recovery during this procedure is shown by the experimental points denoted by the symbol (*) in Fig. 6. These points were measured at station 6 while the tunnel was in operation and some recovery was being obtained. The data points were found to be unique for each flow condition, i. e., mass flow. For no recovery, $p_T = p_6$, whereas recovery will produce $p_T < p_6$. The fact that the pressure just upstream of the first ejector stage appeared to be only a function of the tunnel mass-flow rate is useful when evaluating diffuser performance and is analogous to the exhaust pressure of conventional wind tunnels.

The pressure at station 6 was obtained by both impact- and static-pressure probes, and although scatter was present in the data, subsonic flow was indicated at this station. The data for this measurement shown in Fig. 6 are averages of several points. It should be noted that the data correspond to the optimum setting of the ejector controls. Values other than those shown could be achieved at ejector settings other than the optimum or by bleeding air into the tunnel.

5.0 DISCUSSION OF DIFFUSER THEORY AND EXPERIENCE

Diffuser studies normally concern either open-jet or closed-jet wind tunnels. This classification arises from the fact that the flow process and mechanism of pressure recovery is believed to be completely different in the two cases. Open-jet wind tunnel diffuser performance has not been as extensively studied as that of the closed-jet tunnels. However, for many practical considerations, a facility such as Tunnel L is normally constructed as an open-jet tunnel.

Closed-jet tunnel diffuser performance has been reported extensively in the literature. Such studies as Refs. 6 through 10 provide extensive background in the performance of various diffusers with closed-jet wind tunnels. Several early supersonic wind tunnels were constructed as open-jet facilities, and some studies of diffusers in these facilities have been made. The best known of these is the theoretical and experimental work of Hermann (Refs. 11 and 12). Other early work was done by Ramm (Refs. 13 and 14). Common to all such studies is the presence of low Mach number flow, or high Reynolds number flow, or both, as compared to the flow regimes in the tunnel used for this study. More recent work is reported in Refs. 15 through 18. Reference 18 is a discussion of the state-of-the-art and an attempt to define the more important parameters affecting diffuser performance in the low-density regimes.

In recent years, supersonic diffusers have been used in conjunction with the exhaust nozzles of rocket engines to provide additional pumping action in altitude rocket test facilities. Experience with these systems, which in some cases bear remarkable resemblance to the configuration of Tunnel L, has been reported extensively (Refs. 19 through 28).

5.1 NATURE OF TEST CHAMBER PRESSURE CONTROL

The physical process by which the flow in the diffuser acts to control the test chamber pressure is not completely understood. Various explanations have been attempted, and several are summarized here to provide an insight into the subject. In this regard, several comments are made in Section 7.0 concerning the results of the present investigation. It should be kept in mind that all available theories make basic assumptions which are unrealistic in the flow regime of Tunnel L.

The one-dimensional, inviscid theory given in Refs. 11 and 12 predicts that the test chamber control is a function of the diffuser throat

diameter for a given nozzle exit diameter, diffuser inlet diameter, and Mach number. The theory predicts that, except for the case of test chamber pressure being below a finite limit which is less than nozzle exit static pressure, the flow will become subsonic shortly after entering the diffuser. After becoming subsonic, the flow will be accelerated within the convergent part of the diffuser. If the pressure downstream is low enough, the flow will attain sonic velocity in the throat section. Subsonic velocity will again be reached downstream of the diffuser exit. The theory further predicts that a unique diffuser throat size will result in a balance between test chamber pressure and free-stream pressure. If the throat is made smaller, $p_T > p_\infty$. Conversely, a larger throat size will result in $p_T < p_\infty$. The pressure control considered in this theory is independent of the downstream pressure as long as it is low enough so that sonic flow in the diffuser throat is maintained.

If the level of the test chamber pressure is low enough, a supersonic solution is obtained. In this case, the convergent section of the diffuser causes a deceleration of the supersonic flow with pressure rise. The resulting flow, which contains large boundary layers and oblique shocks, is not amenable to one-dimensional, inviscid analysis.

Several investigations have indicated that pressure control is obtained by pressure transfer through the subsonic boundary layer. In the analysis described above, which is based on thin boundary layers and negligible losses by friction, such pressure transfer is disregarded.

More recent experimental and theoretical work has been conducted by Lee and Von Eschen (Refs. 15 and 16). Their analysis is based on a supersonic air injector theory. The stagnation pressure ratio across the tunnel, as well as the diffuser throat area, was found to contribute to the pressure control.

As a flow model, the theory of Refs. 15 and 16 considers one-dimensional, inviscid, supersonic flow being injected into a constant area mixing region (diffuser) with a perfect subsonic diffusion downstream of the point of conversion to subsonic flow. This flow model leads to the conclusion that the function of a diffuser in a free-jet wind tunnel is merely that of a duct which permits the aspiration effect of the nozzle jet to control the test chamber pressure, and the only function of the diffuser throat is the limiting effect it has on the ratio p_T/p_∞ when sonic flow exists in the throat.

Several theories discussed in conjunction with the behavior of rocket altitude test facilities will be reviewed in Section 8.0.

6.0 EXPERIMENTAL RESULTS WITH NO BLOCKAGE

For purposes of discussion, the results of the present investigation have been divided into the broad classifications of clear and blocked tunnel flow, i. e., without and with a model in the test section, respectively. This emphasizes the practical necessity of studying the case with a model in the tunnel test section. Unless otherwise noted, all data presented will correspond to a clear tunnel.

The chief dependent variable is taken to be the test chamber pressure, or some pressure ratio, rather than the more common diffuser efficiency parameter which compares the pressure recovery to that of a normal shock at the test section Mach number.

6.1 EFFECTS OF VARIABLES STUDIED

An attempt has been made to separate the different variables in order to study the influence of each. However, this was not always possible. The large quantity of data and limitless number of configurations possible require some severe restrictions on the data recorded and presented. Typical data are used to illustrate various points, and brief comments are made about the data recorded but not shown herein.

6.1.1 Free-Jet Length

Each diffuser configuration was adjusted to achieve a range of free-jet lengths (FJL) which could be varied from zero to approximately 28 in., the latter being roughly 7 to 14 nozzle exit diameters, depending on the nozzle used.

Figure 7 shows typical results from this investigation. It may be seen that a FJL about six times the nozzle diameter is a good compromise under these conditions. Inspection of Fig. 7 indicates that the improvement with increasing FJL for the higher mass-flow rates outweighs the slight decrease in recovery for the lower mass-flow rates as the FJL is increased past $FJL/D_1 = 6$.

The results indicated in Fig. 7 are representative in general for all diffusers investigated with the exception of flow condition 4 and the optimum diffuser throat area for that condition which resulted in a reversal of the trend indicated in Fig. 7 (see Fig. 10f). An appraisal of data available to the author reveals that for $6 \lessapprox FJL/D_1 \lessapprox 12$, no great change in recovery resulted, but in some cases with $FJL/D_1 < 6$, a decrease in diffuser efficiency was found to occur.

6.1.2 Diffuser Throat Dimension

Each diffuser was constructed with an entrance diameter of 9.0 in. Since the two nozzles employed in the investigation had different exit diameters, the parameter A_1/A_2 varied between conditions 1, 2, and 3, 4. This parameter and others are listed in the following table for each flow condition.

Flow Condition	A_1/A_2	A_1/A_3	A_2/A_3
1 and 2	0.212	0.269 to 4.297	1.266 to 20.250
3 and 4	0.0494	0.0625 to 1.000	1.266 to 20.250

The diffusers of 2- and 4-in. throat diameters were obtained by placing inserts into one of the 30-deg inlet sections. This resulted in these particular diffusers having no finite minimum-area length or shock duct.

Figure 8 shows typical variation in the pressure ratio, p_T/p_o, as the throat area was varied. These data represent a constant free-jet length and inlet section angle, but the throat or shock duct length varied from 3 to 9 in. This latter effect will be shown to be small over this range in most cases. Shown also is the pressure ratio achieved by the diffuser action of the 10-in. movable pipe. A FJL of 20 in. was chosen as being typical in the normal operation of the tunnel.

As can be seen, an optimum diffuser throat area is indicated for each flow condition. Diffuser throats larger or smaller than these optimum values result in an increasing pressure ratio. The advantage of employing a diffuser is quite apparent. It should be kept in mind that the movable 10-in.-diam pipe itself produces some recovery and is therefore not a true base for measuring the pressure recovery.

A series of experiments with diffuser components 180 and 180M indicated that a slightly different optimum area might be expected with α_i other than 30 deg. Since the effect of throat length, inlet section angle, and free-jet length must be included in overall diffuser performance, the data in Fig. 8 should not be interpreted as representing unique design points for diffuser throat areas at the flow conditions of Tunnel L. Rather, they indicate that changes in diffuser throat area are important in producing recovery if other variables are held constant.

6.1.3 Inlet Section

Several experimental diffuser investigations have shown that the entrance section of a supersonic diffuser is quite important. Because

of increased shock strength and possible boundary-layer interaction, a sharp reduction in area in this region could be expected to produce larger losses than a gradual reduction.

The three entrance components available were run without any other diffuser components attached to study this effect. Figure 9 shows typical results from this investigation. The same trend was indicated for all four flow conditions tested. It appears that the more gentle contraction is advantageous, and one would assume that $\alpha_i < 15$ deg would prove superior to those tested, particularly for small free-jet lengths. Included in Fig. 9 is the length of each entrance component.

6.1.4 Role of Diffuser Components in Pressure Recovery

Several diffuser series were run at each of the four test conditions with separate and combined components to study the role of each component in pressure recovery under significantly varying flow conditions.

The results of these experiments are shown in Fig. 10. Several important results indicating diffuser performance in the low-density regime are illustrated in this figure, and some discussion is warranted. Figure 10a illustrates data taken with a diffuser with a throat area at or near the optimum for flow condition 1. The data reveal that, for $D_3 = 7.0$ in., an increase of throat length from 0 to 9 in. results in a small but measurable improvement in recovery. Also shown are data with the optimum throat area ($D_3 = 8.0$ in.) and contraction angle ($\alpha_i = 15$ deg) which resulted in the highest recovery for flow condition 1. Figure 10b shows that, for the same flow condition but a diffuser throat area not near the optimum, no improvement with increasing throat length is found. Apparent from these figures is the fact that the diffuser inlet component, which also determines the throat area, provides the greatest part of the recovery. Figure 10c reveals the same effect of throat length at a throat cross-sectional area near the optimum for condition 2. The data in Fig. 10d were taken with the optimum inlet and using long throats to study the effect of throat length for $L_t \leq 87$ in. It is seen that no additional recovery is provided for $L_t \geq 18.5$ in., but recovery decreases for $L_t < 18.5$ in. Figure 10e reveals no increase in recovery for $0 \leq L_t \leq 9$ in. and a slight decrease for $L_t = 87$ in. with the flow set at condition 3. However, diffuser throat diameter was not at the optimum value. With the flow set at condition 4, a large improvement in recovery is obtained by increasing the throat length as is shown in Fig. 10f. This improvement resulted even though the throat area was greater than the optimum for this particular flow condition. In this case the inlet section is of secondary importance, with the effect of throat length providing the primary recovery.

No increase in recovery was provided by the addition of a subsonic diffuser when $L_t \leq 9$ in. However, no subsonic diffusers were tested with $L_t > 9$ in.

7.0 NATURE OF THE FLOW IN THE DIFFUSER

In order to improve understanding of the physical mechanism by which the test chamber pressure is controlled, it was thought helpful to study the flow process within the diffuser.

The shock system existing between the nozzle exit and diffuser inlet is easily explained and can be predicted qualitatively by simple inviscid theory for overexpanded and underexpanded nozzle flow. The same statement cannot be made about the flow model within the diffuser because of the complex interaction between the central flow and the boundary layer.

Conventional flow visualization systems commonly used in supersonic wind tunnels are not suitable in Tunnel L because of low densities. However, when the tunnel is operated with argon at high total temperatures, there is a natural flow visualization thought to be caused by radiation from relaxing metastable argon atoms. The flow condition referred to as condition 3 in the present investigation is one with which this natural visualization exists.

Figure 11 shows the nozzle shock system discussed earlier for two different test chamber pressures. An impact-pressure probe placed on the nozzle centerline also detects this shock system and is the normal method used to map the flow. To continue the survey of the flow process into the diffuser, probes were constructed which could be inserted into the diffuser throat and controlled by the probe carrier. Both lateral and centerline surveys were possible using these probes.

Diffuser configuration 26-6+16-36 was selected to be surveyed, and tubes for measurement of static pressure were attached to the wall as shown in Fig. 5. No significant decrease in pressure recovery was noted with the addition of these tubes which were well submerged in the thick boundary layer. Typical results from this series of experiments are shown in Figs. 12 and 13. These results are indicative of all flow conditions studied.

Because of the reaction of the shock system to pressure changes, it was found that the results were very sensitive to small variations in test chamber pressure. Therefore, every effort was made to keep pressures constant.

Small tufts of nylon thread attached to diffuser configuration 180-0+0-0 revealed a marked flow reversal in the vicinity of the diffuser inlet plane (Fig. 14).

Wall static and centerline impact probes installed in the diffuser components with $L_t \geq 15.5$ in. revealed that subsonic velocities had been reached for large values of FJL and L_t. The diffuser exit Mach number appeared, however, to be primarily a function of the distance from the nozzle exit to the diffuser exit and nearly independent of diffuser throat length or diameter.

From examination of results illustrated in Figs. 11 through 14, the flow model shown schematically in Fig. 15 can be inferred and the following conclusions drawn:

1. The flow appears to remain supersonic throughout the entire diffuser, except with large FJL and L_t, with subsonic flow appearing at some station downstream of the diffuser but upstream of station 6.
2. The shock system in the central core of flow is indicated by pressures on the diffuser wall only as a smooth, gradual pressure rise because of an extremely thick boundary layer.
3. Large impact pressure gradients are present across any given cross section of the diffuser.
4. The flow process near the inlet plane of even the shallowest diffuser inlet is complex because reversed flow is present. Presumably a still less abrupt contraction would alleviate this.
5. The physical mechanism of the phenomena observed is much like that of an ejector with no secondary flow and a second throat (diffuser) which produces an aspiration effect, thereby controlling the test chamber pressure.

8.0 ANALYSIS OF THE EXPERIMENTAL RESULTS

Diffuser flows have never been successfully treated by a theoretical approach except with simplifications which generally involve neglect of viscous fluid effects. A theoretical approach invariably is reduced to a qualitative discussion of the expected trends in the data, and it is apparent that viscous influences cannot be neglected in the present case. Both the complex flow model and the need to confine the scope of the present investigation to a practical limit precludes

either a theoretical or broadly valid empirical approach at the present time. However, a discussion of the results with comparison to similar but high-density facilities is useful.

8.1 PRESSURE RATIOS AVAILABLE IN TUNNEL L

The starting and operating pressure ratios which are of common interest in conventional wind tunnel diffuser investigations are of no special interest in the present case. Tunnel pressure ratio p_o/p_6 provided by the ejector system is sufficient to produce shock-free flow at the nominal test section. The additional pumping action of the diffuser is used to produce further expansion of the nozzle flow, thereby increasing the simulation capabilities of the tunnel. The method of operation whereby the tunnel is evacuated to a low pressure before flow is introduced through the aerodynamic nozzle also serves to eliminate starting problems.

Diffuser recovery represented by the increase in nozzle pressure ratio and the corresponding increase in Mach number is shown in Fig. 16. An order of magnitude improvement is seen to exist for each of the flow conditions studied during the present investigation. Included in Fig. 16 are data representing no recovery ($p_T = p_6$) and the optimum, i. e., lowest p_T. The diffuser configurations yielding these optimum recoveries are listed in Table 2.

8.2 FREE-JET LENGTH AND DIFFUSER INLET ANGLE

The experimental data obtained during the present investigation indicate that an increase of FJL up to approximately six nozzle exit diameters and a decrease in α_i resulted in increased diffuser recovery. Both of these trends have been observed by several investigators (e. g., Refs. 16, 20, 21, 24, and 25).

At small values of the FJL the flow from the nozzle exit impinges on the diffuser inlet wall, thereby causing an increase in the static pressure in the diffuser inlet. Even at large values of the FJL it was found that the wall pressure gradient was greater in the inlet section than throughout the rest of the diffuser (Fig. 12). An added effect may arise from the physical presence of the supersonic nozzle in the vicinity of the diffuser inlet for small FJL. This would tend to effectively block the diffuser and hinder the aspiration of gas from the test chamber. The slight decrease in recovery for FJL $\gtrsim$ 6 could be caused by the viscous mixing loss along the free-jet boundary.

The advantage of having a gradual inlet section slope for increased diffuser recovery in normal, higher density flows is well known. Shock strength and boundary-layer separation effects dictate such a configuration. The strong reversed flow in the vicinity of the inlet plane and its interaction with the supersonic core and wall boundary layer should also be reduced somewhat if α_i were reduced in the present case.

8.3 AREA RATIO EFFECTS

The variation of test chamber pressure with changes in diffuser throat diameter is of primary importance in the present case. In addition to the theories discussed in Section 5.1, other approaches have been attempted (Refs. 23, 26, 29, and 30) to explain variations in test chamber pressure as determined by diffuser throat diameter when configurations having $A_3 > A_1$ are involved (see Fig. 17). The simplest of these (Refs. 23 and 26) involves the assumption that $p_T = p_\infty$, defined by a Mach number corresponding to isentropic expansion for the area ratio A_3/A^*.

A two-dimensional, mixing-layer theory for compressible turbulent jet mixing derived by Korst, Chow, and Zumwalt (Ref. 29) and discussed by Goethert (Ref. 30) for application in the solution for base pressures on rockets with jet exhausts is of interest. A strong influence of nozzle exit flow angle, θ_n, and ratio of specific heats, γ, is shown by the mixing-layer theory. The theory is not considered reliable at values of $p_T/p_o < 0.0020$, and its direct application in the present case would be of little use. The method is based on the fact that the base pressure is determined by the mixing profile in the boundary zone of the jet and assumes in its simplest form that the mixing layer starts with zero thickness at the nozzle exit. The presence of the nozzle boundary layer, of course, violates this assumption. The effect of the boundary layer is to increase the base pressure above that predicted by the theory since, in effect, the boundary layer is adding additional mass flow to the test chamber.

A collection of data reported in the literature is shown in Fig. 17, with data from the present investigation, to illustrate the diffuser area ratio effect. The data selected represent the optimum recovery (lowest p_T) for each diffuser throat diameter. Each point denotes a condition for which the nozzle and diffuser flow was established and therefore should be independent of exhaust pressure. Also, only data with $\theta_n \cong 15$ deg and $\gamma = 1.4$ were selected from the references. The present data include $\gamma = 1.67$ as well as 1.4. Plotting pressure ratios obtained when $A_3/A_1 >$ optimum, as shown in Fig. 8, would cause the data to depart from the trend indicated in Fig. 17; thus these data were omitted from Fig. 17.

The present results plotted as a function of the actual physical area ratio A_3/A^* are seen to fall considerably above the majority of the data from other facilities. If it is assumed that

A_3/A_1 with boundary layer = A_3/A_1 without boundary layer

and

A_1/A^* = area ratio defined by the calibrated Mach number at the nozzle exit rather than the nozzle geometry

and the data plotted accordingly, much better agreement is obtained. This again emphasizes the importance of the boundary layer in determining the effective area ratios.

The correlation is by no means perfect, as might be expected considering the many differences between various configurations, but the presentation does indicate the influence of the diffuser throat below the limit where further enlargement is a disadvantage. It does not indicate the throat dimension at which test chamber pressure begins to rise, and consideration of overall diffuser performance must also include starting and operating pressure ratios.

8.4 DIFFUSER THROAT LENGTH

The compression process involves a series of conical shocks whose strength and number are functions of the entering flow conditions and diffuser geometry. In the Mach number range of Tunnel L a throat or shock-duct length on the order of 15 throat diameters may be required for the compression process to reduce the flow to subsonic velocities. Even with effective diameters much less than the actual physical diameters, caused by thick boundary layers, the length required is large, and the fact that the flow continues to be supersonic throughout diffusers of short length should not be surprising. An examination of Fig. 10 leads to the conclusion that the throat length may be important in obtaining optimum pressure recovery, and its influence appears to increase with increasing Reynolds number. The reduction of the flow to subsonic velocity at the diffuser exit does not appear, however, to be necessary or sufficient for optimum recovery. Identical recovery was obtained with M_4 being subsonic, transonic, or supersonic in the series of experiments illustrated in Fig. 10d.

9.0 PRESSURE RECOVERY

The efficiency parameter listed in Table 2 follows the definition and analysis of Hermann (Ref. 11) and compares the entropy increase throughout the diffuser to that of a normal shock at the test section Mach number.

The entropy increase and diffuser efficiency can be related to the ratio of total pressures before and after the diffuser losses by the following equations:

$$K_{diff} = p_{o_6}/p_{o_2} = e^{-\left(\frac{S_{o_6}-S_{o_2}}{R}\right)} \tag{1}$$

$$\eta_D = K_{diff}/K_{NS} = \frac{p_{o_6}/p_{o_2}}{(p_o'/p_o)_{NS}} \tag{2}$$

If all losses downstream of the test section which is bounded on its downstream end by station m are considered as part of the overall diffuser system, then Eq. (2) may be reduced to

$$\eta_D = \left(p_{o_6}/p_{o_m}\right)\Big/\left(p_o'/p_o\right)_m$$

Since in the inviscid core upstream of the first shock,

$$p_o = p_{o_m}$$

and, from experience with Tunnel L in particular,

$$p_{o_6} \cong p_6$$

Eq. (2) reduces simply to

$$\eta_D = p_6/p_{o_m}' \tag{3}$$

Since p_{o_m}' is a direct function of p_T for a given flow condition and can be determined experimentally, Eq. (3) can be evaluated. Note that p_{o_m}' is the minimum impact pressure in the test section, actually corresponding to vanishing uniform core flow diameter. Thus, its use yields the highest η_D, and the values given are limiting in the present case.

The values of diffuser efficiency listed in Table 2 represent the optimum performance with a clear tunnel. Since the evaluation of Eq. (3) depends on an experimentally determined value of p_{o_m}', and the probe used to measure p_o' partially blocked the flow, the values listed were obtained by extrapolation to the clear tunnel condition. Thus they must be considered approximate. Data taken with $p_T > (p_T)_{min}$ were extrapolated to arrive at the flow conditions existing at the maximum flow expansion point corresponding to $(p_T)_{min}$ with a clear tunnel. The accuracy of the extrapolations is felt to be sufficient to indicate the approximate pressure recovery for the various flow conditions studied.

The optimum recovery for each of the flow conditions of the present investigation is shown in Fig. 18 with diffuser efficiency and tunnel

Reynolds number as the correlating parameters. Shown also are typical ranges of recovery and Reynolds number for conventional higher density facilities with fixed geometry diffusers. The data from the present investigation were plotted using an effective tunnel Reynolds number which takes into account the expansion beyond the nozzle exit and may be expressed by

$$Re_{D_{eff}} = \left[\frac{(A/A^*)_m}{(A/A^*)_{M_1}}\right]^{1/2} (D_1) \left(\frac{Re_\infty}{in.}\right)_m \tag{4}$$

where $(A/A^*)_m$ and $(A/A^*)_{M_1}$ are from the calibrated values of M_m and M_1. It will be recognized that Eq. (4) is based on a finite diameter at station m, comparable to the use of nozzle exit diameter in other collections of data, even through no usable core of flow exists.

Diffuser efficiencies on the order of 100 percent are common for fixed geometry diffusers and facilities with conventional Reynolds number levels. A marked improvement in efficiency is seen to exist with increasing Reynolds number in Tunnel L, which operates at a Reynolds number level several orders of magnitude less than other facilities. The influence of viscous forces as compared to compressibility effects is evident.

10.0 EXPERIMENTAL RESULTS OF BLOCKAGE TESTS

During the first phase of the investigation it was found that the probe placed at station 5 produced, in some cases, a variation in diffuser performance. Since the magnitude of this effect could not be accurately determined, a series of blockage tests was conducted to explore this problem. By definition, Tunnel L is considered blocked when the oblique shock system originating in the vicinity of the nozzle exit focuses on the nozzle axis at a point upstream of the desired test region.

The procedure during the blockage investigation was to place each model 5 or 6 in. downstream of the nozzle exit on the centerline. After desired flow conditions were established, the model was moved upstream to a point 1.0 in. inside the nozzle. The direction of movement was then reversed and the model returned to its original position. The test chamber pressure was recorded at each 1.0-in. increment of model movement. The models were mounted on both the short and long stings shown in Fig. 4 to study the effect of the sting length. This procedure was repeated for each of three diffusers. No attempt is made in the present report to include all of the large amount of data which this procedure yielded. Figure 19 shows typical experimental results.

Examination of Fig. 19 reveals an interesting phenomenon. In several cases when the larger models were placed downstream of the nozzle exit, the tunnel was unable to produce shock-free flow conditions. As the model was moved upstream, a point was reached where the test chamber pressure suddenly decreased and the shock system was re-established downstream. The model could then be returned downstream to a certain extent until the test chamber pressure once again increased and the shock system jumped upstream to its original position. It was found that the sudden reduction in test chamber pressure occurred when the model was positioned at a station which closely corresponded to the centerline intersection (station m) of the nozzle shock system. Also shown in Fig. 19 is the experimentally determined variation in location of the first shock intersection on the centerline at station m as a function of p_T. A model placed sufficiently far upstream of this point can be considered to be in a shock-free test region.

Figure 20 illustrates the effect of model size and shape for several different diffusers and flow conditions. The effect of streamlined models and model supports can be seen. It was found that introduction of blockage actually reduced the test chamber pressure below that of the clear tunnel values in many cases. An examination of the data revealed that for the condition where a reduction in diffuser throat size resulted in a lower test chamber pressure, the addition of the blockage model was beneficial. The opposite was true for the condition where a reduction in throat size caused an increase in test chamber pressure. Thus, the models were acting as centerbody diffusers.

A higher test chamber pressure was created with the shorter model sting. This is illustrated in Fig. 21. The shock interaction with the sting support normal to flow direction is probably the reason for this effect.

The effect of model blockage on diffusers of various throat dimensions can be seen in Fig. 22. Also included are minimum test chamber pressures when no blockage is present.

A comparison of blockage results from the present investigation with those of other supersonic tunnels would not be meaningful unless effective areas accounting for boundary-layer thicknesses were used (cf., Ref. 1, Fig. 15). It was found in Ref. 31 that relatively larger models could be used in tunnels with extremely high pressure ratios. This seems to be confirmed by the present results.

11.0 CONCLUDING REMARKS

The basic results and conclusions of this investigation of diffusers in Tunnel L can be summarized as follows:

1. The widely held opinion that, because of large viscous losses, a diffuser would not be of use in a facility of this type was shown to be erroneous in Ref. 1 and further confirmed by the new results reported here.

2. The physical mechanism of the phenomena observed is similar to that occurring in an ejector with no secondary flow and with a second throat (diffuser) which produces an aspiration effect, thereby controlling the test chamber pressure.

3. For a given supersonic flow condition and tunnel exhaust pressure, it was found that diffuser throat area was the dominant parameter in determining test chamber pressure, with variations in diffuser inlet contraction angle, throat length, and free-jet length being of secondary importance.

4. A decrease in test chamber pressure resulted as diffuser throat area was increased up to a limiting throat area. Beyond this optimum throat area, the test chamber pressure increased.

5. Diffuser throat length was found to become increasingly important in obtaining pressure recovery as viscous effects decreased, i. e., as Reynolds number increased.

6. A series of tests to determine the effect of blockage on pressure recovery revealed that, for model sizes up to the maximum allowed by the size of the uniform core in the nozzle, the recovery could be maintained or improved by the presence of the model if adjustments in diffuser throat area were made.

7. Although pressure recovery, as compared to that in conventional tunnels, was found to be small because of large viscous losses, the benefit of even this small recovery in increasing nozzle pressure ratios and decreasing cost of the pumping system was significant.

8. It is believed that the results of this investigation may be applied to the design of fundamentally similar wind tunnels and propulsion test facilities. In particular, Fig. 18 is a guide to the performance which may be expected when low Reynolds numbers are involved.

REFERENCES

1. Potter, J. L., Kinslow, M., Arney, G. D., Jr., and Bailey, A. B. "Description and Preliminary Calibration of a Low-Density, Hypervelocity Wind Tunnel." AEDC-TN-61-83. August 1961.

2. Potter, J. L. and Boylan, D. E. "Experience with an Over-expanded Nozzle in a Low-Density, Hypervelocity Wind Tunnel." AEDC-TDR-62-85, April 1962.

3. Boylan, D. E. "An Analysis of Initial Static Pressure Probe Measurements in a Low-Density Hypervelocity Wind Tunnel." AEDC-TDR-63-94, April 1963.

4. Potter, J. Leith, Arney, George D., Kinslow, Max, and Carden, William H. "Gasdynamic Diagnosis of High-Speed Flows Expanded from Plasma States." IEEE Transactions on Nuclear Science, Vol. NS-11, No. 1, January 1964, pp 145-147.

5. Lewis, A. D. and Arney, G. D., Jr. "Vibrational Nonequilibrium with Nitrogen in Low-Density Flow." AEDC-TDR-63-31, March 1963.

6. Lukasiewicz, J. "Diffusers For Supersonic Wind Tunnels." Journal of the Aerospace Sciences, Vol. 20, Number 9, September 1953.

7. Neumann, E. P. and Lustwerk, F. "High-Efficiency Supersonic Diffusers." Journal of the Aerospace Sciences, Vol. 18, Number 6, June 1951.

8. Wegener, Peter, P. and Lobb, R. Kenneth. "An Experimental Study of a Hypersonic Wind-Tunnel Diffuser." Journal of the Aerospace Sciences, Vol. 20, Number 2, February 1953.

9. Hermann, R., Leitinger, H., and Melnik, W. L. "Research on the Design of Hypersonic Nozzles and Diffusers at High Stagnation Temperatures." WADC-TN-55-507, March 1955.

10. Johnston, Patrick J. and Witcofski, Robert D. "Effect of a Variable-Geometry Diffuser on the Operating Characteristics of a Helium Tunnel Designed for a Mach Number in Excess of 20." NASA TN D-237, February 1960.

11. Hermann, Rudolf. "Diffuser Efficiency and Flow Process of Supersonic Wind Tunnels with Free Jet Test Section." AF Tech. Rept. No. 6334. December 1950.

12. Hermann, Rudolf. "Diffuser Efficiency of Free-Jet Supersonic Wind Tunnels at Variable Test Chamber Pressure." Journal of the Aerospace Sciences, Vol. 19, Number 6, June 1952.

13. Ramm, Heinrich. "Measurements of the Pressure Distribution in the Entire Wind Tunnel, and Especially in the Diffuser by Means of Small Pressure Gages." GS-AAF-Wright Field No. 20, May 1947.

14. Ramm, Heinrich. "Phenomena in Supersonic Diffusers." GS-AAF-Wright Field No. 43, November 1947.

15. Lee, J. D. and von Eschen, G. L. "An Experimental and Analytical Investigation of Critical Design Parameters for High Mach Number Open-Jet Supersonic Wind Tunnels." Report No. SR-41 for Contract No. W33-038 ac-21683, Ohio State University Research Foundation, March 1954.

16. Lee, J. D. and von Eschen, G. L. "Critical Performance Parameters of an Intermittent High-Pressure Free-Jet Supersonic Wind Tunnel." Final Rept. to WADC Cont. No. W33-038 ac-21683, The Ohio State University Research Foundation, July 1954.

17. Hill, Jacques A. F. "Diffuser Performance in the Open Jet Hypersonic Wind Tunnel." AR Memo No. 243, Massachusetts Institute of Technology, May 1958.

18. Milligan, M. W. and Bailey, J. F. "Low-Density Hypervelocity Wind Tunnel Diffuser Performance." AEDC-TDR-63-30, January 1963.

19. Sandberg-Serrell Corporation. "Altitude Facility Diffuser Study: Variable Area Diffuser Report." Report R446-2 (AD-241293), May 1960.

20. Jones, W. L., Price, H. G., and Lorenzo, C. F. "Experimental Study of Zero-Flow Ejectors Using Gaseous Nitrogen." NASA TN D-203, March 1960.

21. Bauer, R. C. and German, R. C. "The Effect of Second Throat Geometry on the Performance of Ejectors without Induced Flow." AEDC-TN-61-133, November 1961.

22. German, R. C. and Bauer, R. C. "Effects of Diffuser Length on the Performance of Ejectors without Induced Flow." AEDC-TN-61-89, August 1961.

23. Bauer, R. C. and German, R. C. "Some Reynolds Number Effects on the Performance of Ejectors without Induced Flow." AEDC-TN-61-87, August 1961.

24. Taylor, D., Barton, D. L., and Simmons, M. "An Investigation of Cylindrical Ejectors Equipped with Truncated Conical Inlets--Phase II." AEDC-TN-60-224, March 1961.

25. Bauer, R. C., German, R. C. and Panesci, J. H., Arnold Engineering Development Center, Unpublished Data, June 1963.

26. Barton, D. L. and Taylor, D. "An Investigation of Ejectors without Induced Flow - Phase I." AEDC-TN-59-145, December 1959.

27. Foster, Richard M. "The Supersonic Diffuser and Its Application to Altitude Testing of Captive Rocket Engines." AFFTC-TR-60-1, January 1960.

28. Mickola, Richard H. "Performance Summary of the Supersonic Diffuser and Its Application to Altitude Testing of Captive Rocket Engines." Addendum to AFFTC-TR-60-1, April 1961.

29. Korst, H. H., Chow, W. L., and Zumwalt, G. W. "Research on Transonic and Supersonic Flow of a Real Fluid at Abrupt Increases in Cross Section (with Special Consideration of Base Drag Problems)." Final Report University of Illinois, ME-TR-392-5, December 1959.

30. Goethert, B. H. "Base Flow Characteristics of Missiles with Cluster-Rocket Exhausts." Aerospace Engineering, March 1961.

31. Schueler, C. J. "An Investigation of the Model Blockage for Wind Tunnels at Mach Numbers 1.5 to 19.5." AEDC-TN-59-165, February 1960.

32. Makofski, R. A. and Rea, S. N. "A Study of Shock-Duct Diffusers in a Helium Hypersonic Tunnel." Presented at Hypervelocity Technique Symposium, March 17-18, 1964, Denver Research Institute, Denver, Colorado.

TABLE 1
TEST CONDITIONS

Flow Condition Number	$\dot{m}$, lb_m/hr	D*, in.	L_n, in.	θ_n, deg	D_1, in.	$(r_{e.c.})_1$, in.	δ_1, in.	Test Gas	p_o, psia	T_o, °K	H_o, Btu/lb_m	x, in.	M_∞	p_∞, μHg	Re_∞/in.	λ_∞, in.
1	4.43	0.113	11.0	9°36'	4.146	1.06	1.56	N_2	17.79	3050	1586	0	9.13	41	530	0.0261
												3	9.64	29	450	0.0324
												6	10.12	21	390	0.0394
2	6.80	0.113	11.0	9° 36'	4.146	1.18	1.38	N_2	22.50	2070	1033	0	9.57	38	990	0.0144
												3	10.09	26	850	0.0178
												6	10.61	19	745	0.0208
3	9.55	0.405	2.98	15	2.00	0.77	0.35	A	2.25	3000	672	0	5.83	220	1290	0.00747
												3	8.18	45	864	0.0154
												6	9.81	19	742	0.0222
4	19.3	0.405	2.98	15	2.00	0.82	0.29	A	3.24	1500	333	0	6.07	263	4650	0.00219
												3	8.97	44	3390	0.00320
												6	11.02	16	2830	--

TABLE 2

OPTIMUM DIFFUSER PERFORMANCE

Flow Condition Number	Optimum Diffuser Configuration	Optimum FJL, in.	Minimum p_T, μHg	$(M_\infty)_m$	$\frac{(Re_\infty)_m}{\text{in.}}$	$(p_o')_m$, μHg	p_6, μHg	η_D, % [Eq. (3)]
1	180M-0+25-0	3	6	12.2	220	1150	210	18.3
2	180-8+7C-0	5	14	12.7	440	1180	285	24.2
3	180-8+18-0	7	21	12.9	650	1210	320	26.5
4	180-8+7G-0	7	33	16.5	2100	850	530	62.4

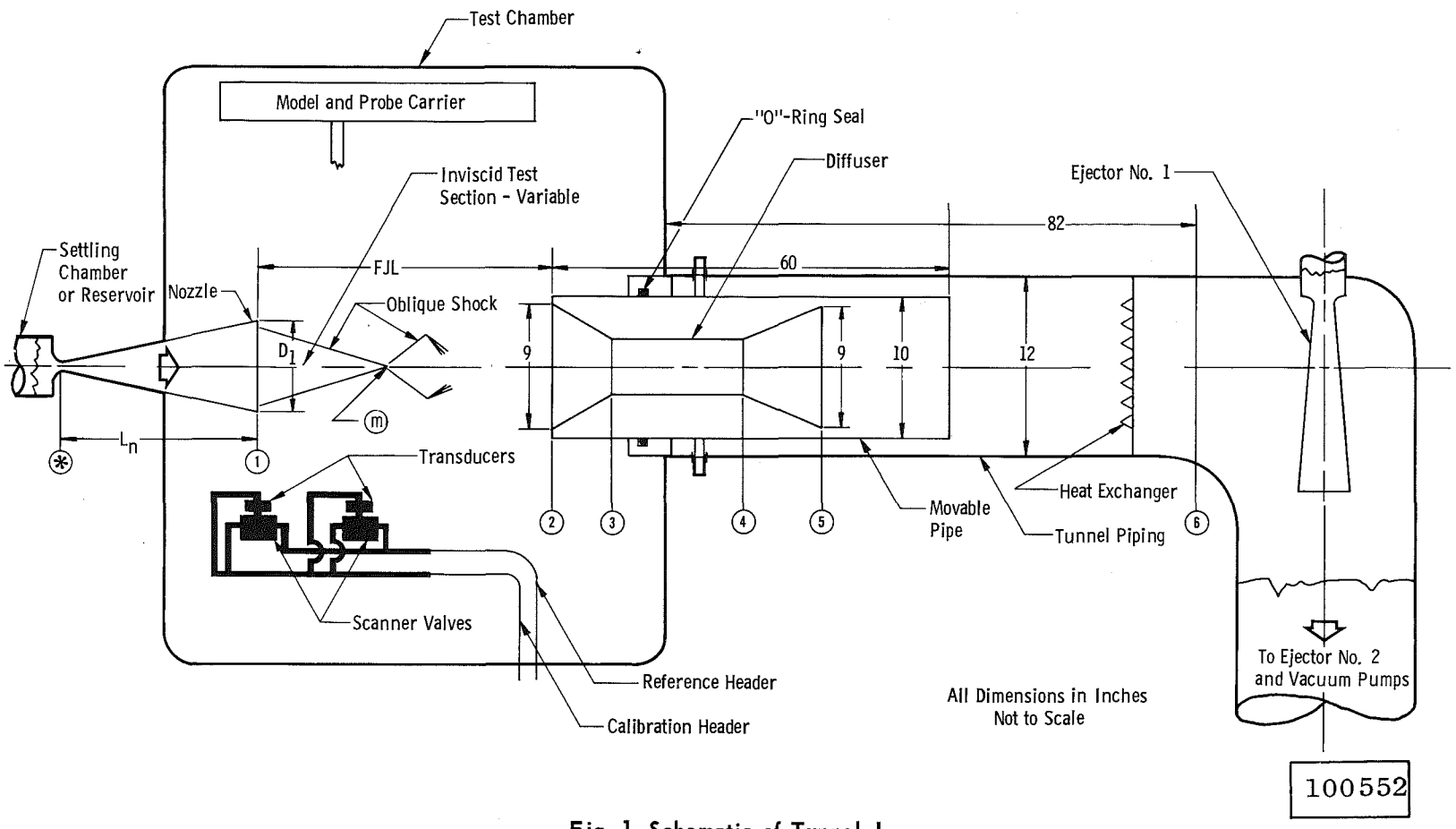

Fig. 1 Schematic of Tunnel L

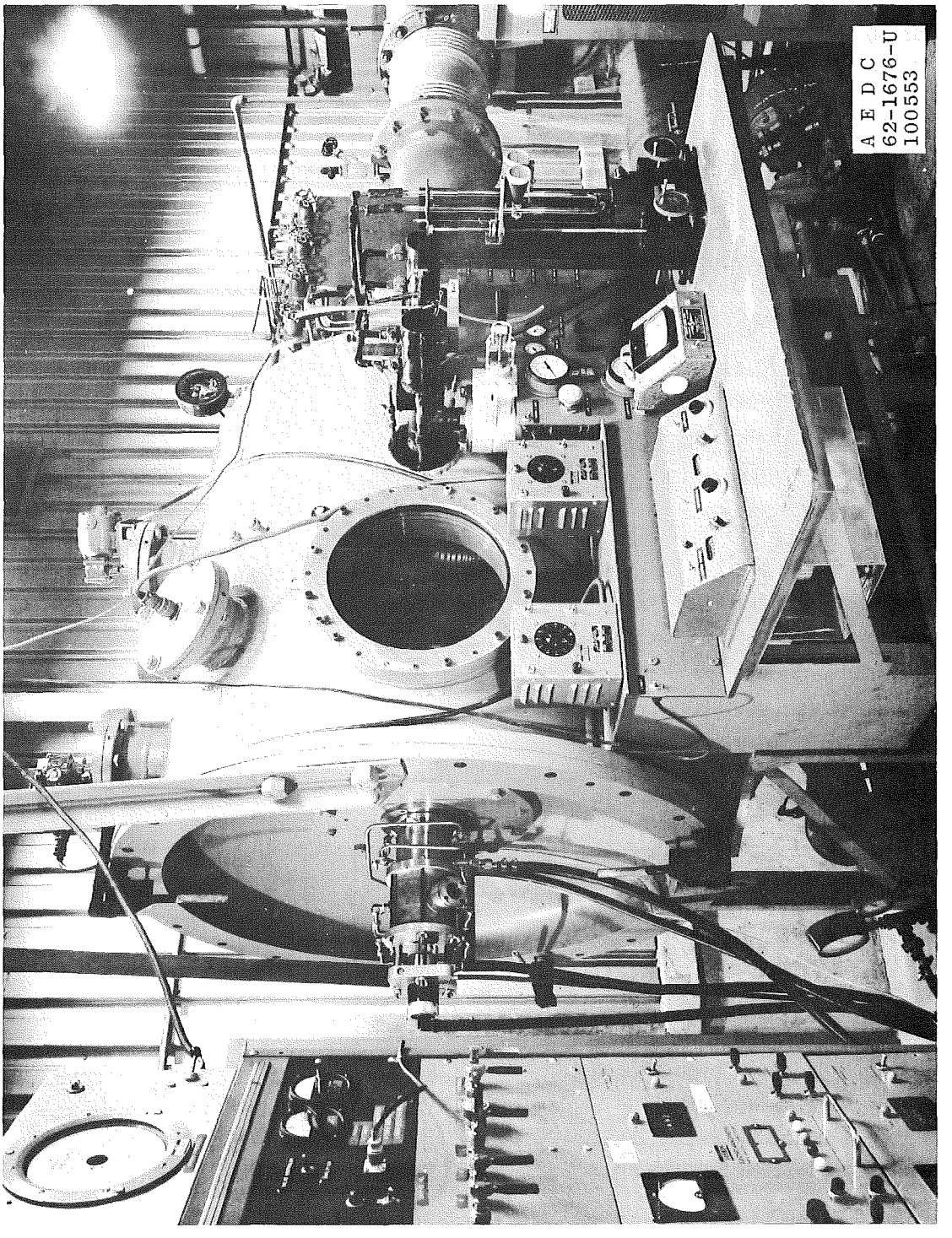

Fig. 2 Photograph of Tunnel L from the Operator's Side

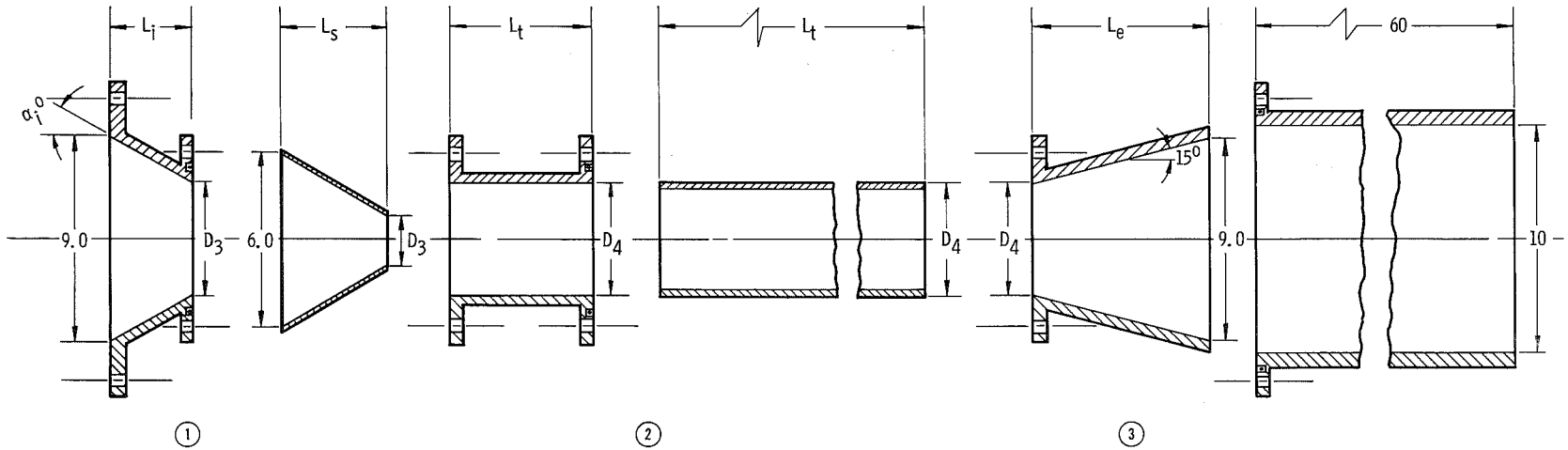

Inlet Components

No.	D_3	L_i	α_i^o
26	5.0	3.46	30
28	5.5	3.03	30
30	6.0	2.59	30
32	6.5	2.16	30
34	7.0	1.73	30
178	5.5	1.75	45
180	5.5	6.53	15
180M	8.0	1.86	15

Material - Stainless Steel

Inserts

No.	D_3	L_s
A	4	1.7
B	2	3.5

Material - Brass Shim

Throat Components

No.	D_4	L_t
6	5.0	3.0
8	5.5	3.0
10	6.0	3.0
12	6.5	3.0
14	7.0	3.0
16	5.0	6.0
18	5.5	6.0
20	6.0	6.0
22	6.5	6.0
24	7.0	6.0

Material - Stainless Steel

No.	D_4	L_t
7C	5.5	15.5
7D	5.5	26.0
7E	5.5	38.0
7F	5.5	60.0
7G	5.5	84.0
25	8.0	72.0

Material - Stainless Steel
0.031 Wall

Exit Components

No.	D_4	L_e
36	5.0	7.46
38	5.5	6.53
40	6.0	5.60
42	6.5	4.67
44	7.0	3.73

Material - Stainless Steel

Movable Pipe
Material - Steel

Dimensions Are in Inches.

100554

Fig. 3 Diffuser Components

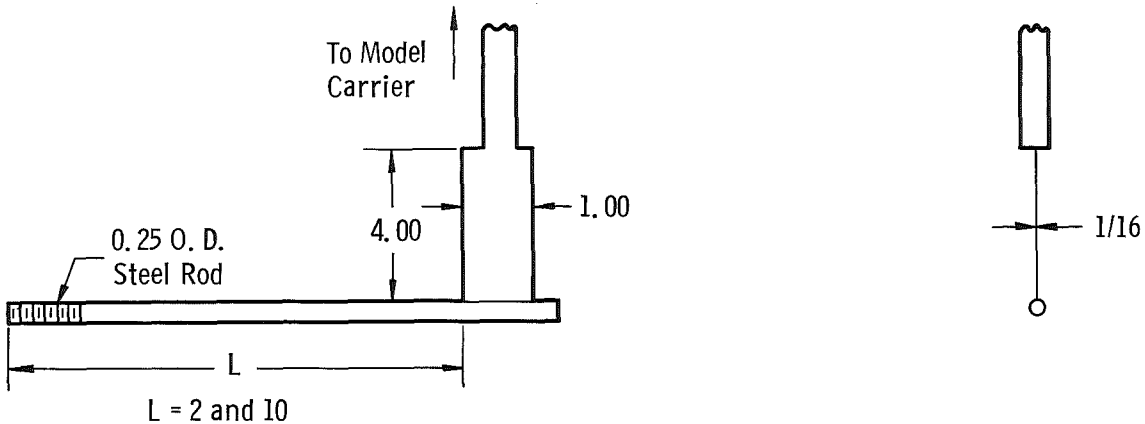

Blockage Model Stings

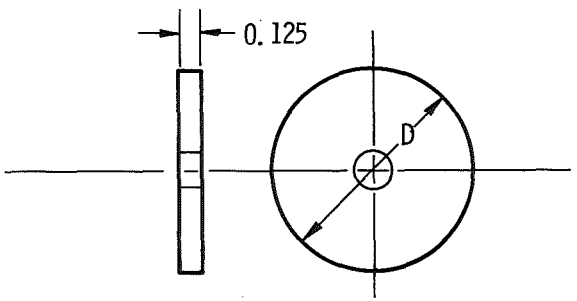

Blunt Models

Material-Brass

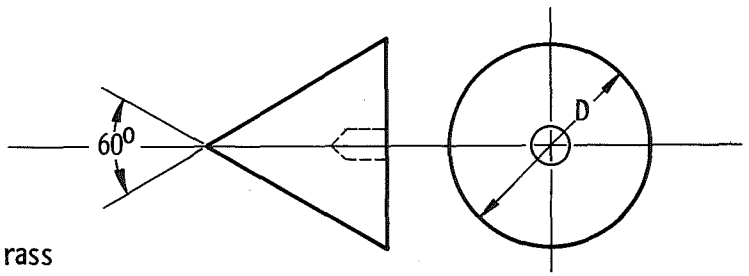

Sharp Models

Model No.	1-B	2-B	3-B	4-B	5-B
D	0.5	0.75	1.00	1.25	1.50

Model No.	1-S	2-S	3-S	4-S	5-S
D	0.5	0.75	1.00	1.25	1.50

Dimensions Are in Inches.

100555

Fig. 4 Blockage Models

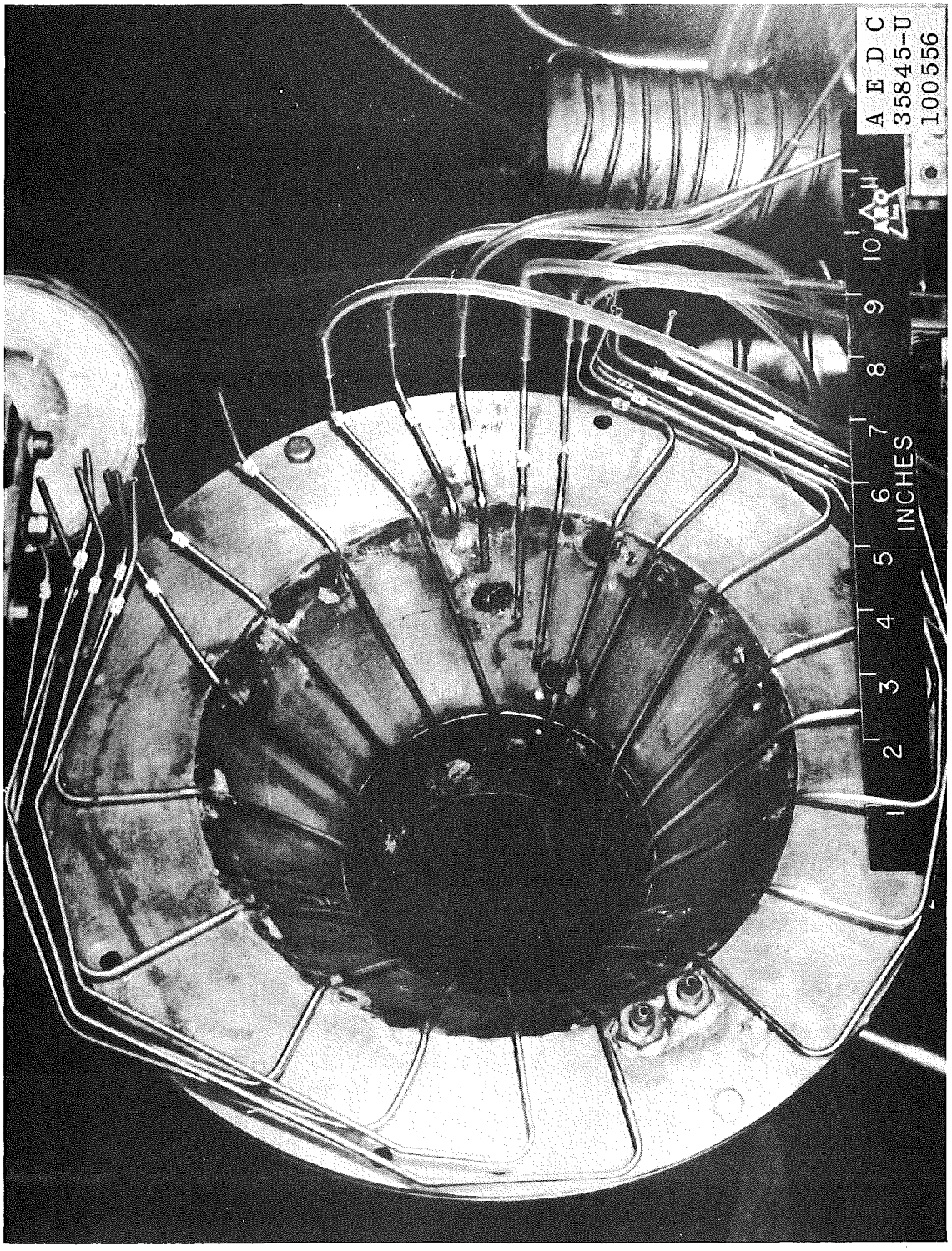

Fig. 5 Diffuser with Wall Static-Pressure Tubes Installed in Tunnel

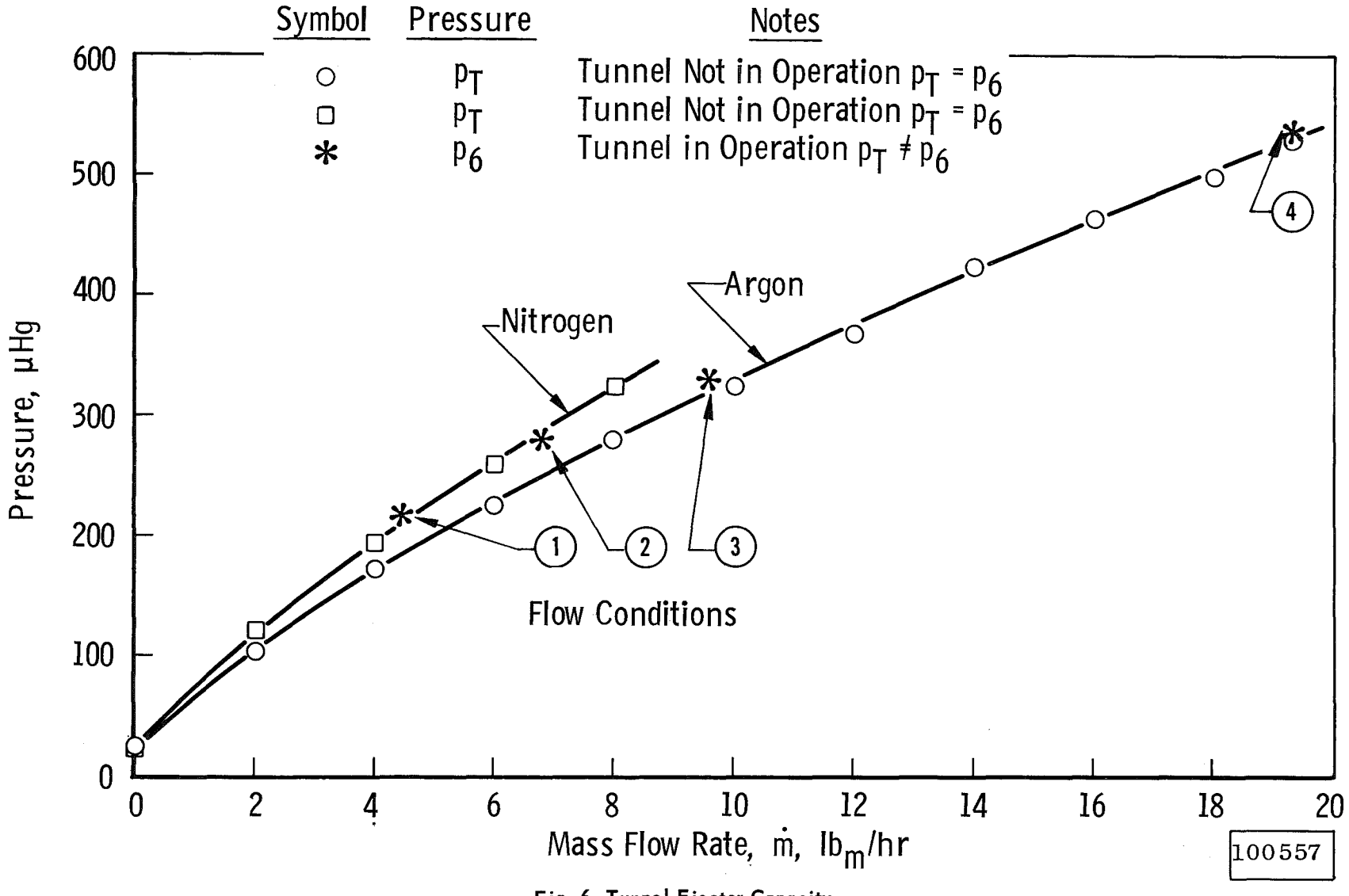

Fig. 6 Tunnel Ejector Capacity

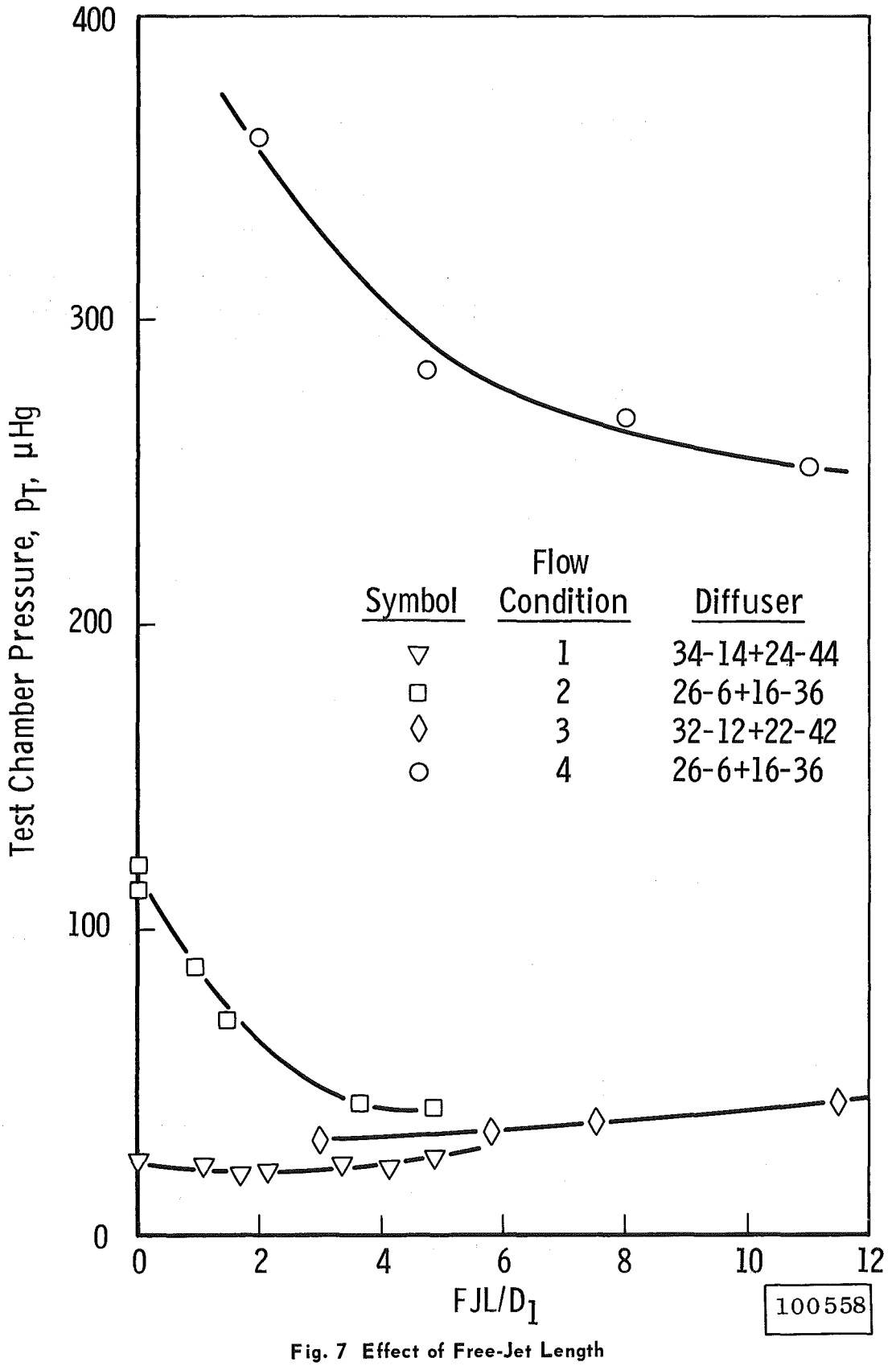

Fig. 7 Effect of Free-Jet Length

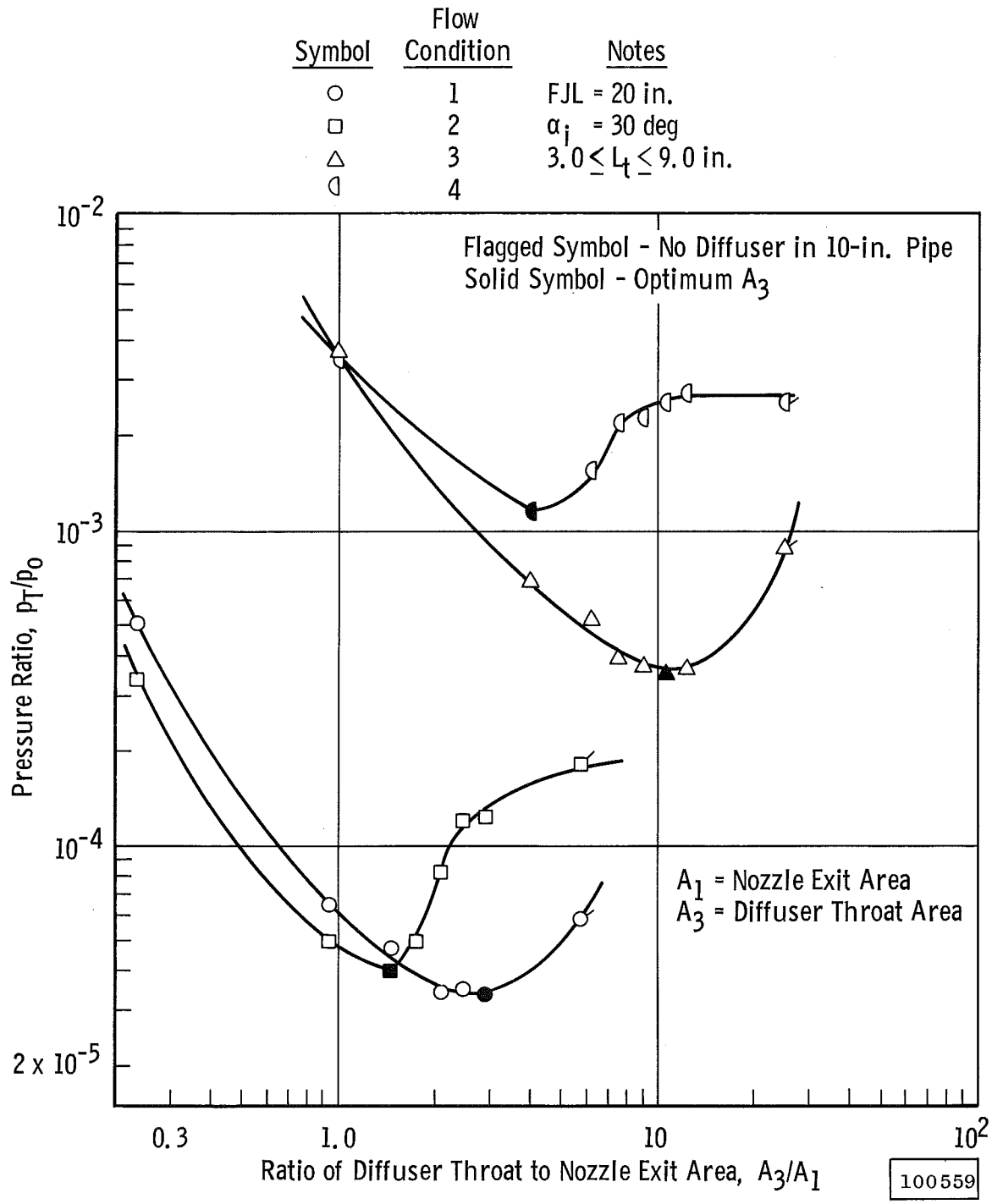

Fig. 8 Effect of Diffuser Throat Area

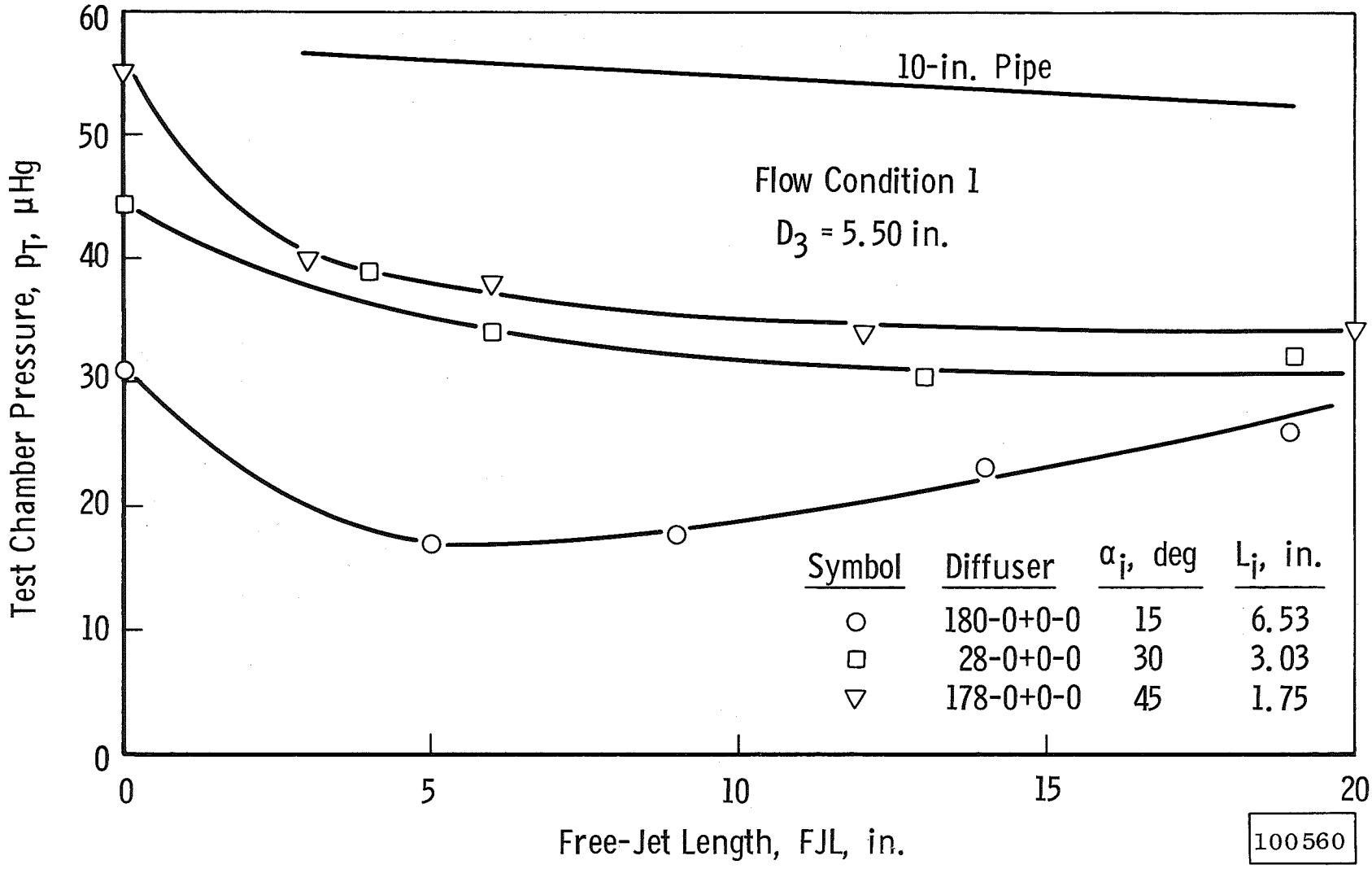

Fig. 9 Effect of Inlet Section Angle

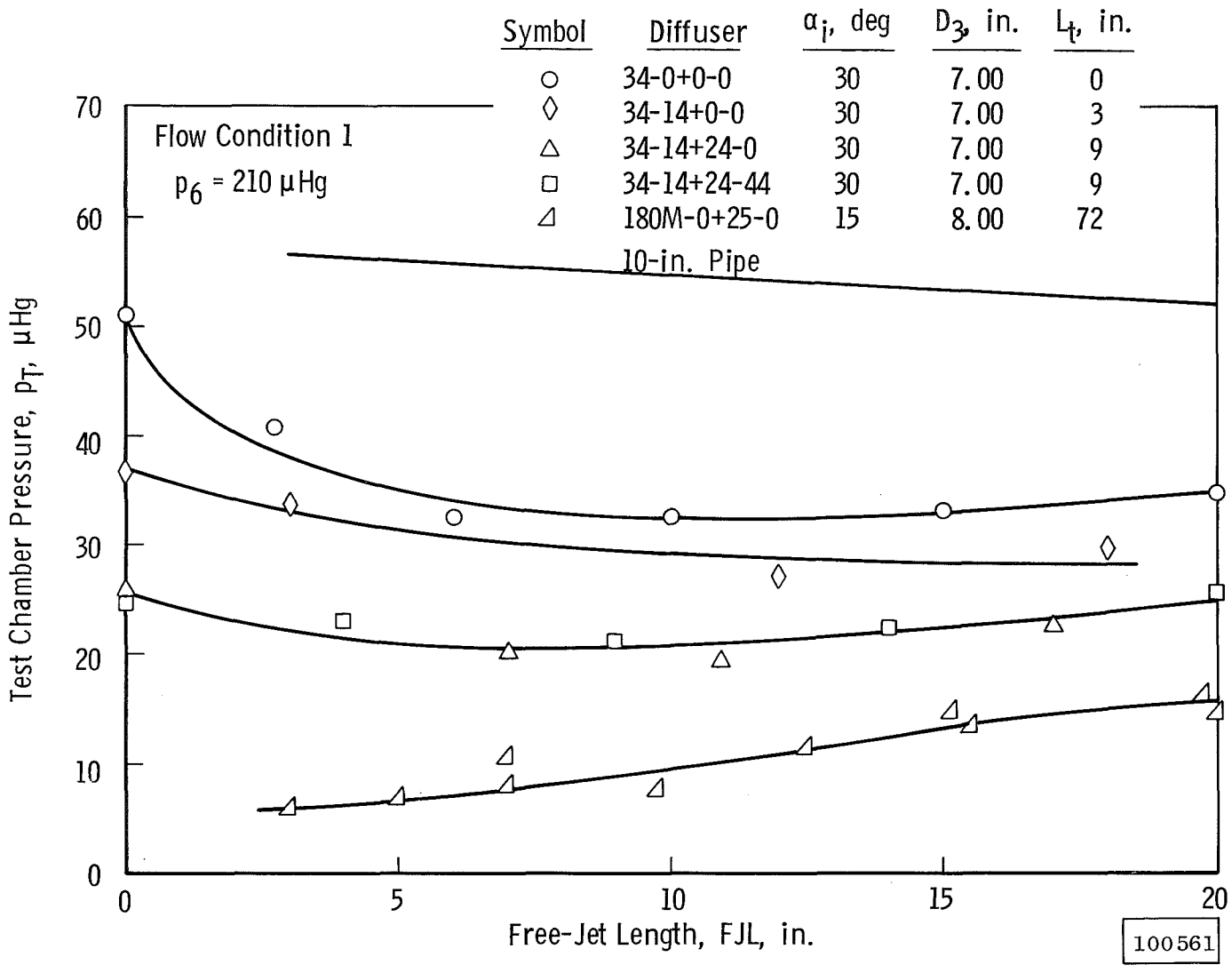

a. Diffuser Throat Area at or Near Optimum (Flow Condition 1)

Fig. 10 Effect of Diffuser Components

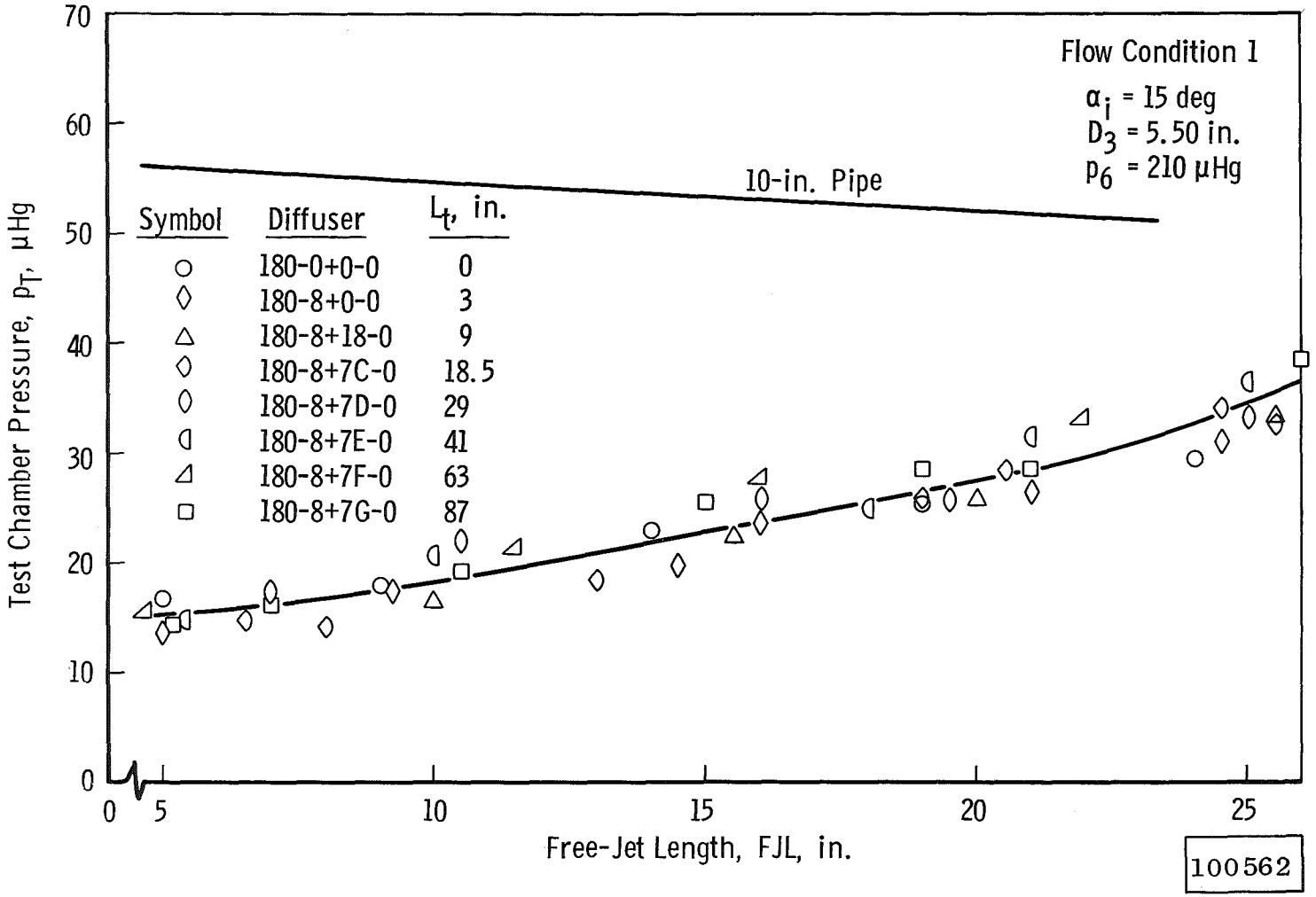

b. Diffuser Throat Area Not Near Optimum (Flow Condition 1)

Fig. 10 Continued

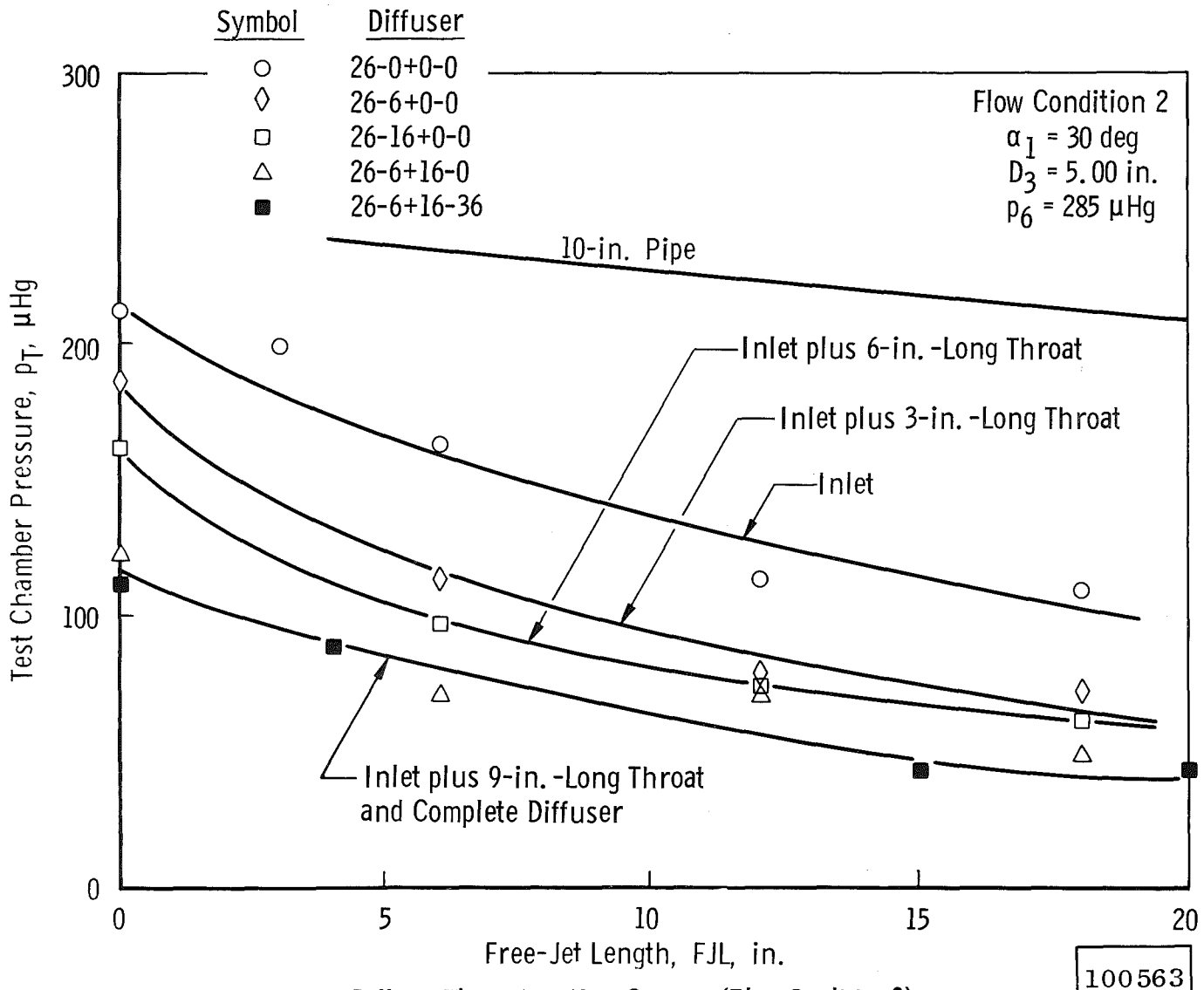

c. Diffuser Throat Area Near Optimum (Flow Condition 2)

Fig. 10 Continued

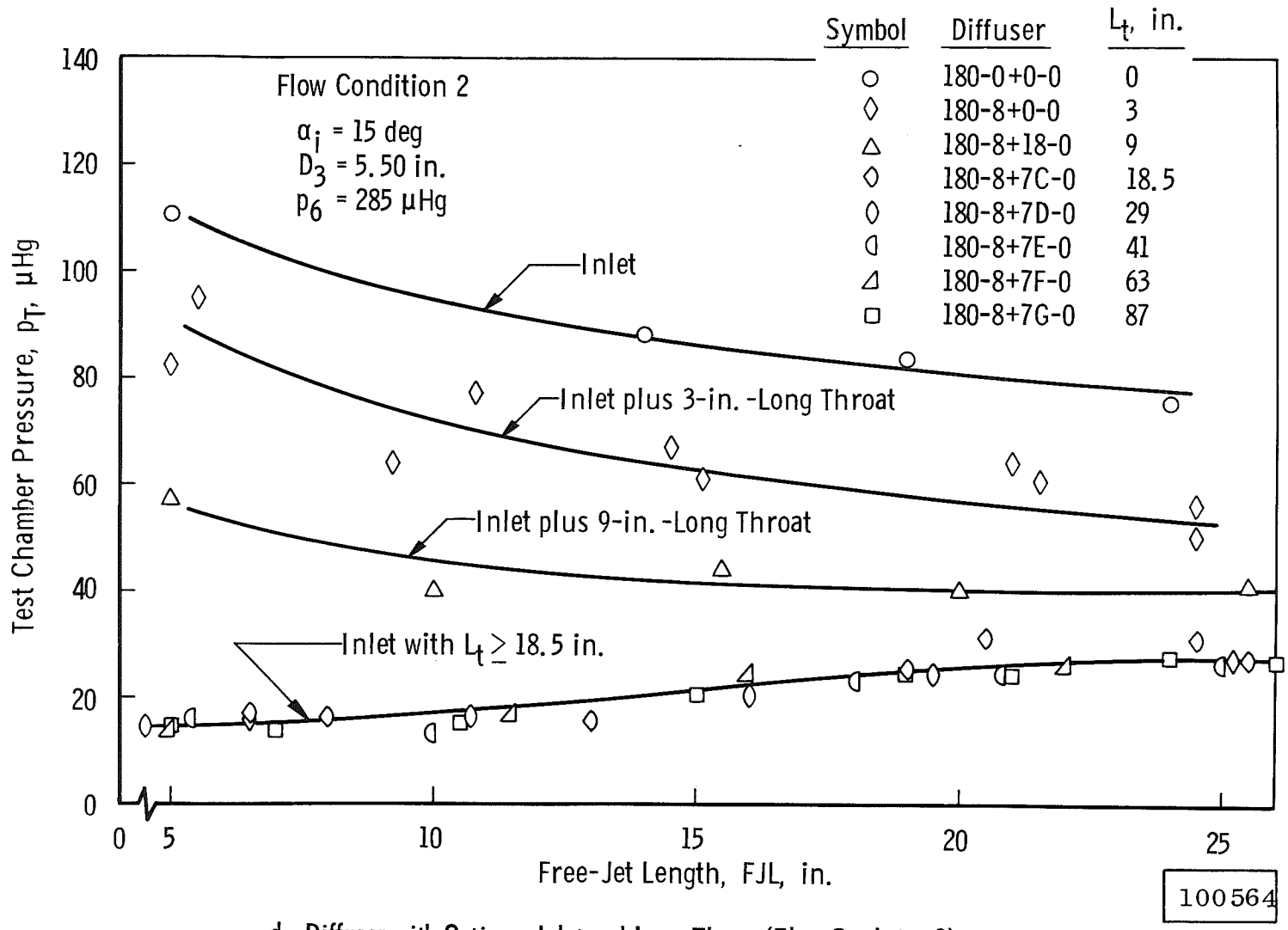

d. Diffuser with Optimum Inlet and Long Throat (Flow Condition 2)

Fig. 10 Continued

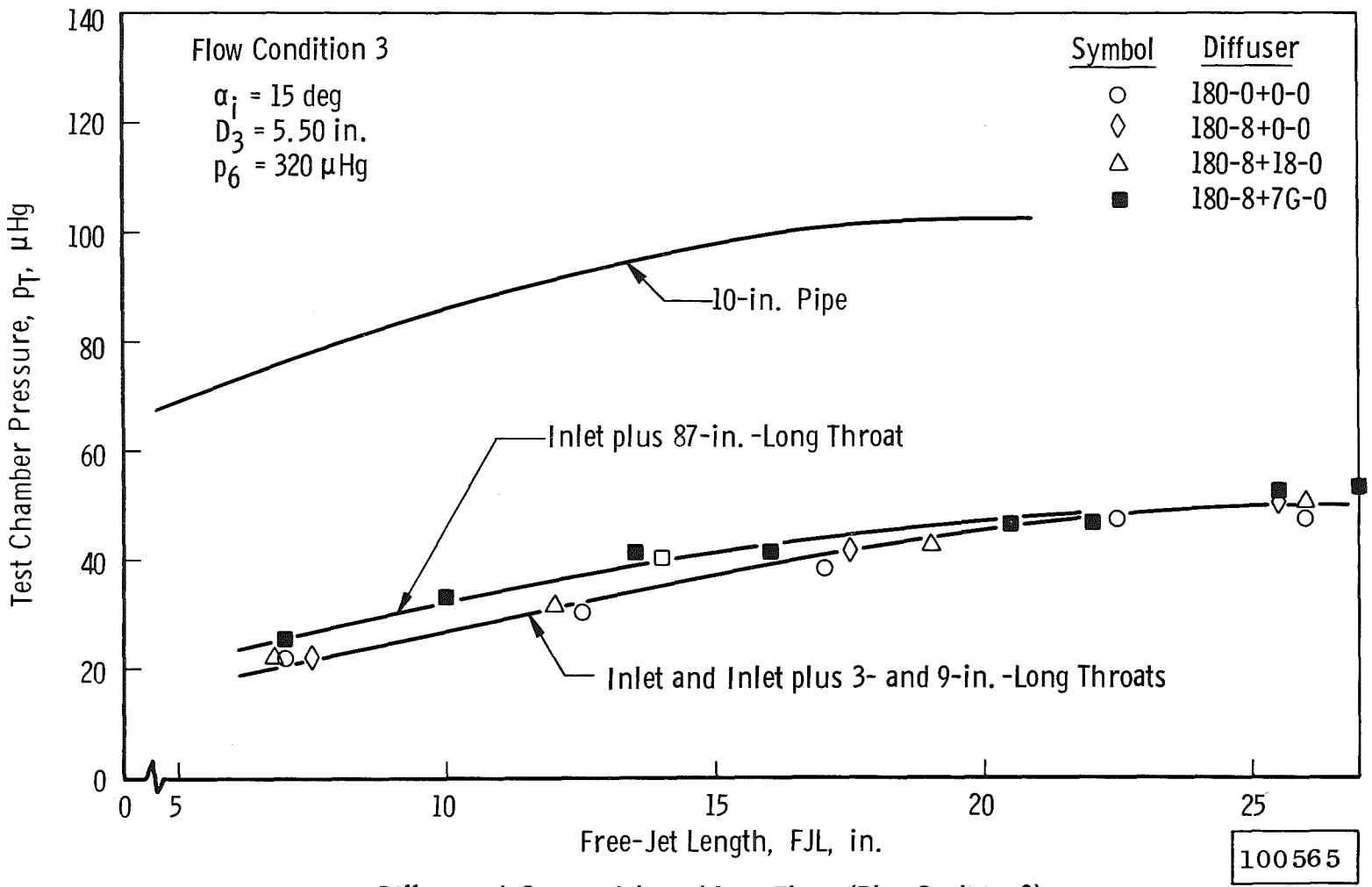

e. Diffuser with Optimum Inlet and Long Throat (Flow Condition 3)

Fig. 10 Continued

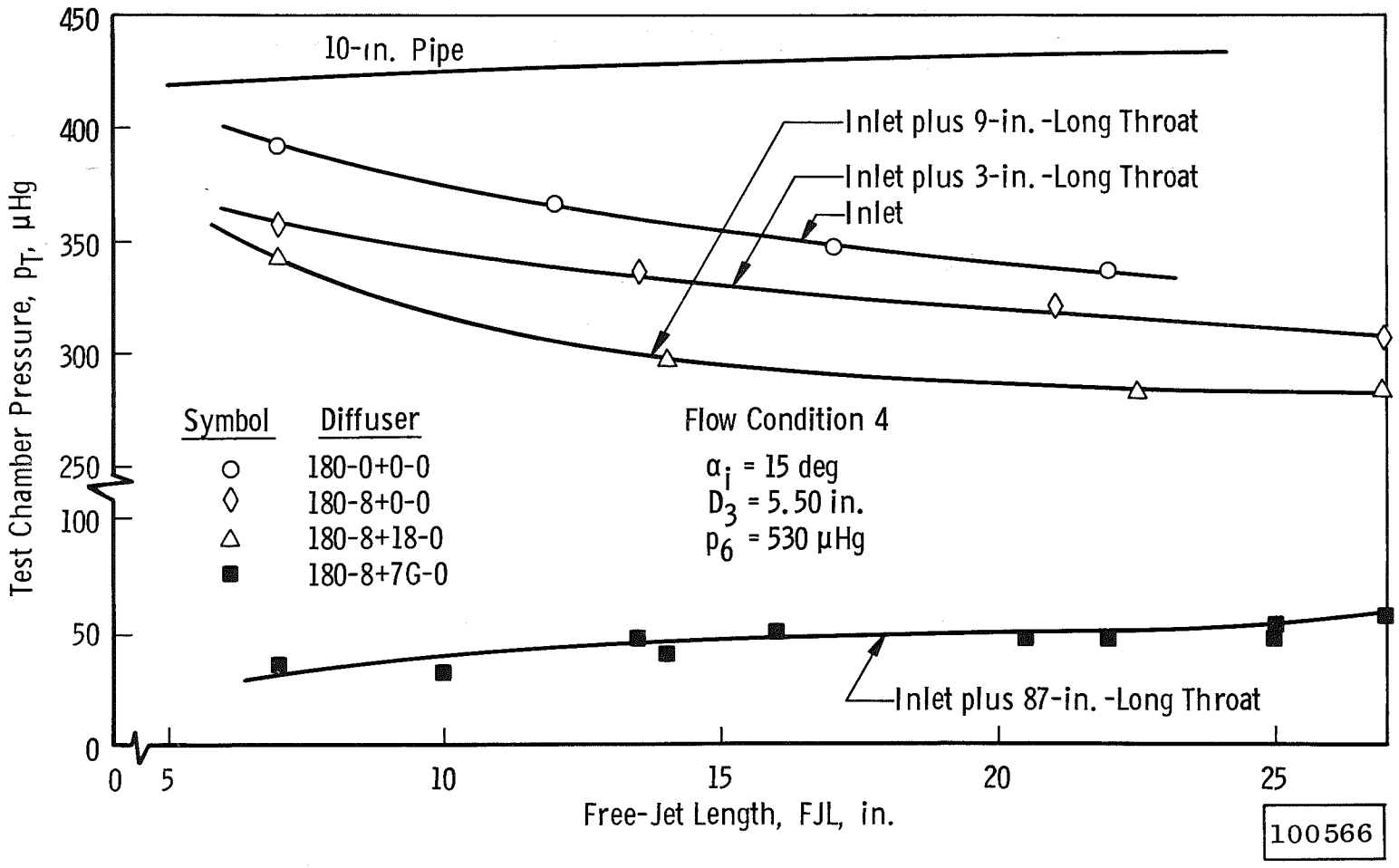

f. Diffuser with Optimum Inlet and Long Throat (Flow Condition 4)

Fig. 10 Concluded

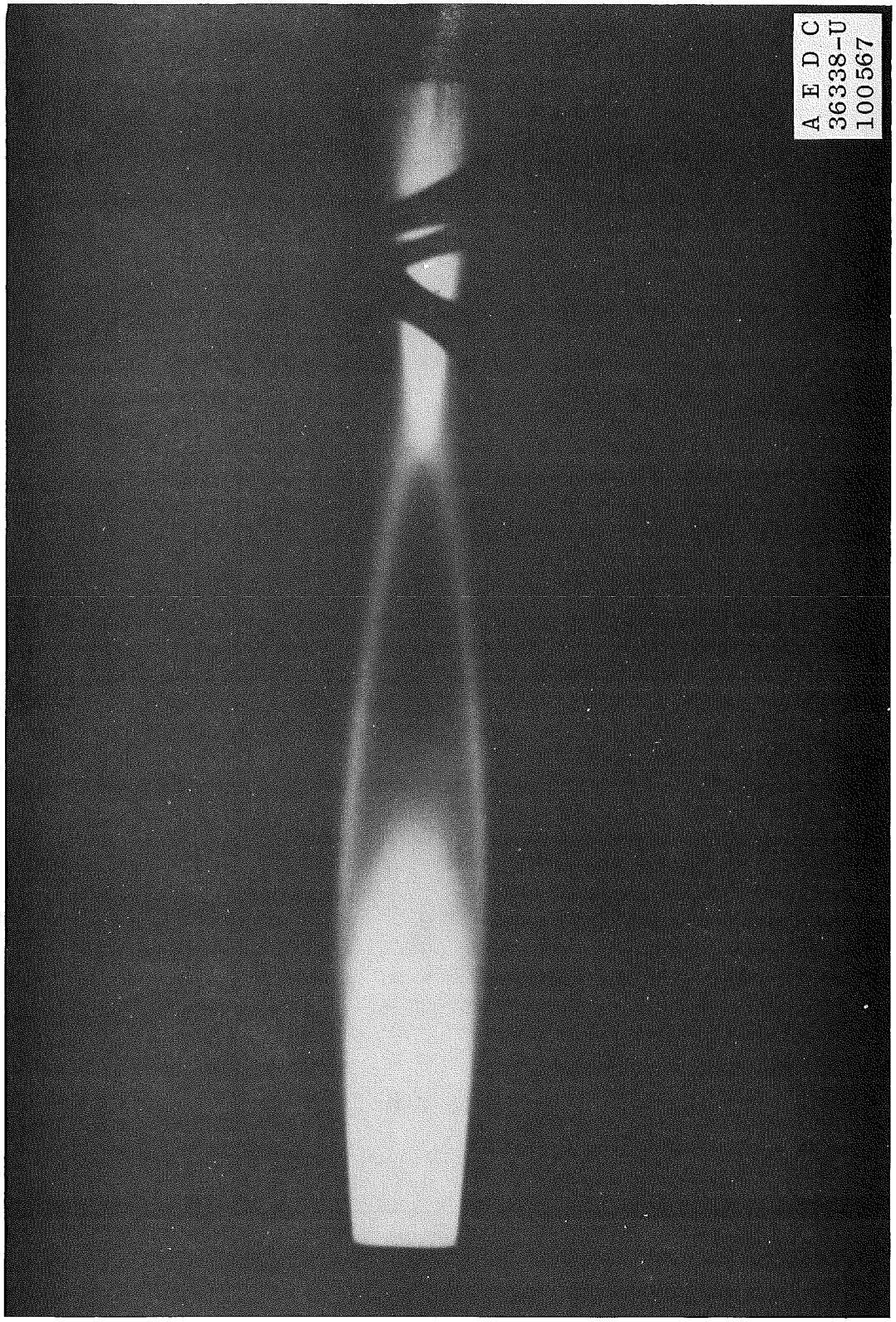

a. Flow Condition 3, $p_T \cong 110\ \mu$ Hg, $p_\infty \cong 220\ \mu$ Hg

Fig. 11 Nozzle Shock System Revealed by Natural Flow Visualization

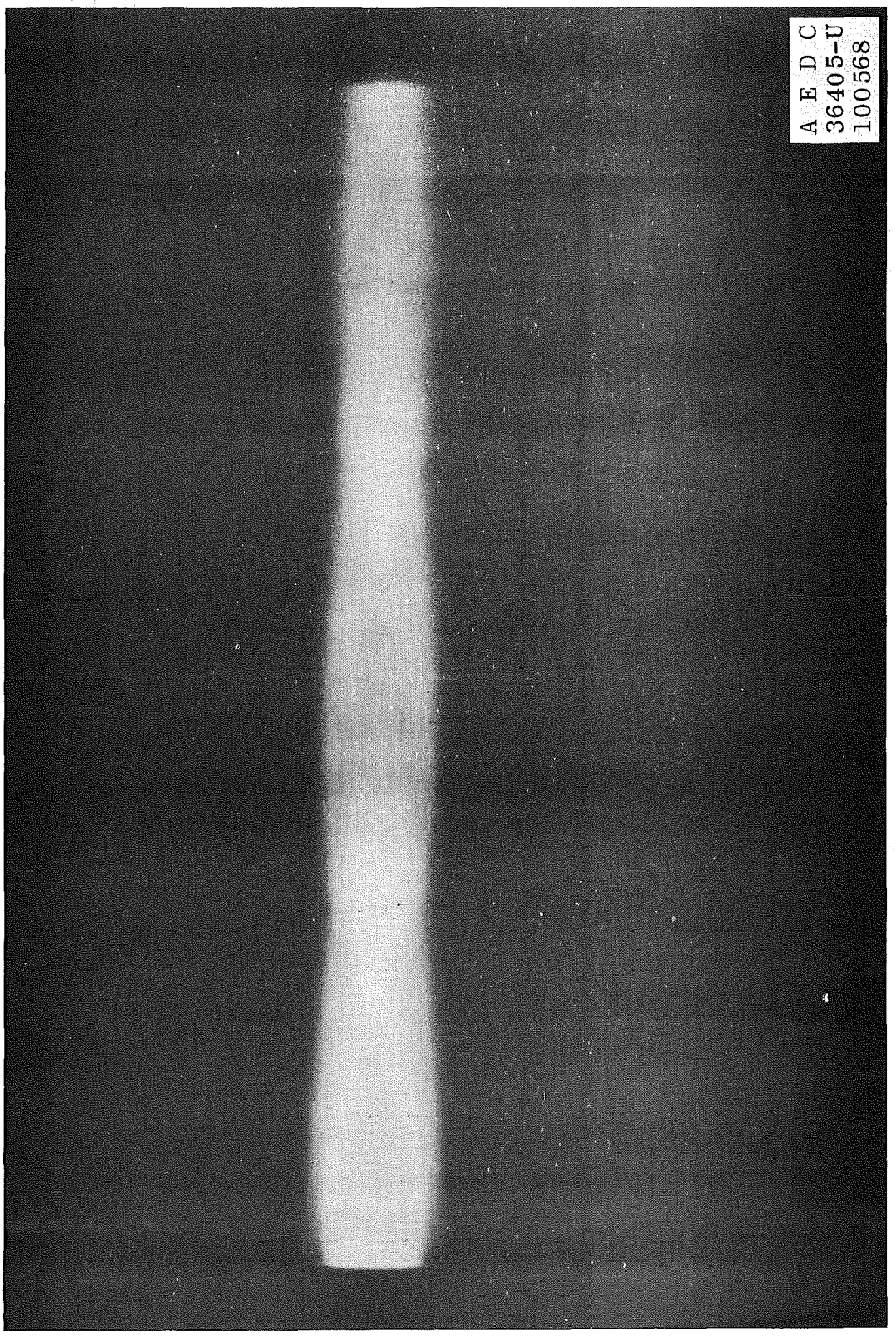

b. Flow Condition 3, $p_T \cong 550\ \mu$ Hg, $p_\infty \cong 220\ \mu$ Hg

Fig. 11 Concluded

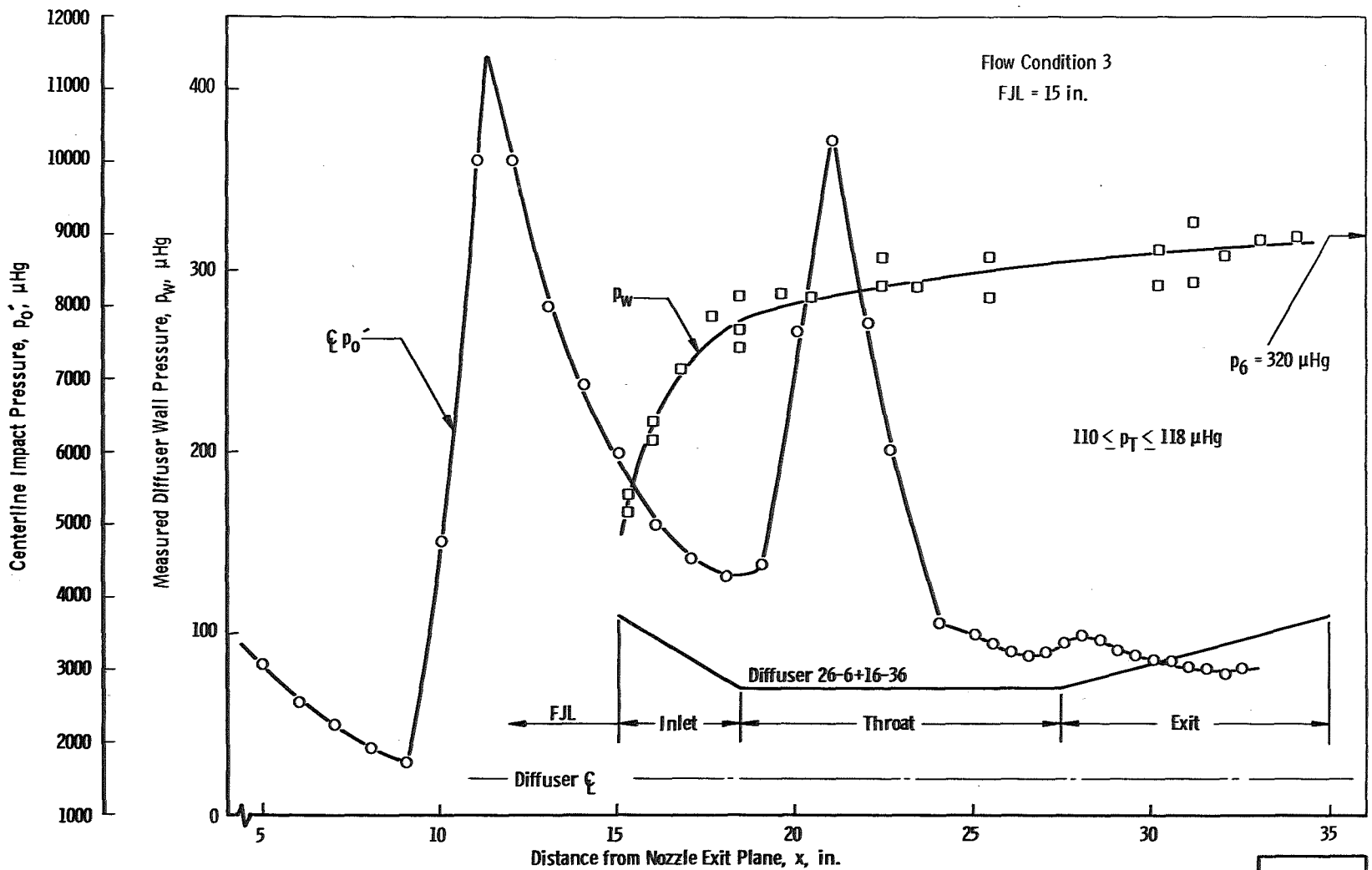

Fig. 12 Centerline and Wall Pressure Surveys

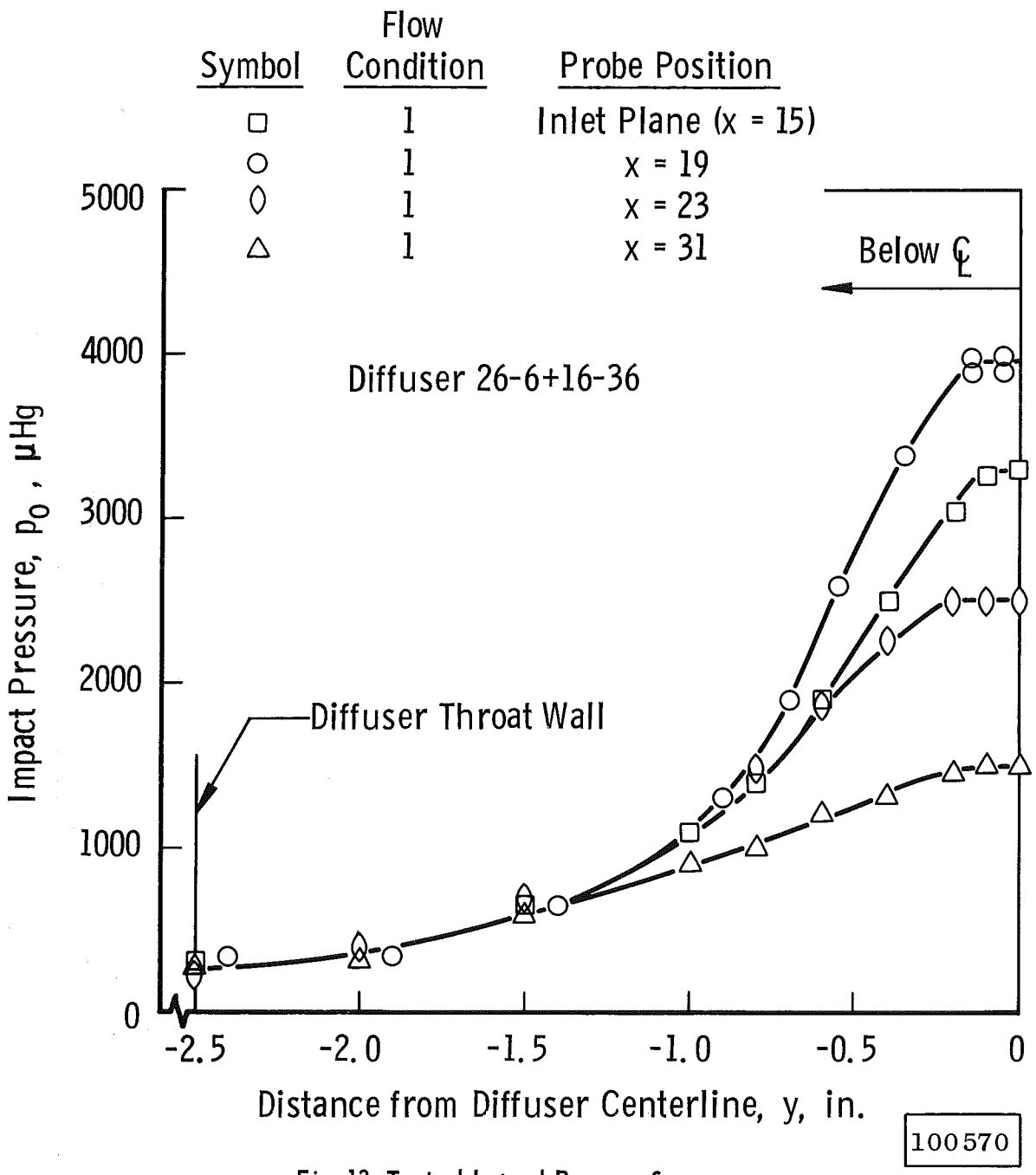

Fig. 13 Typical Lateral Pressure Surveys

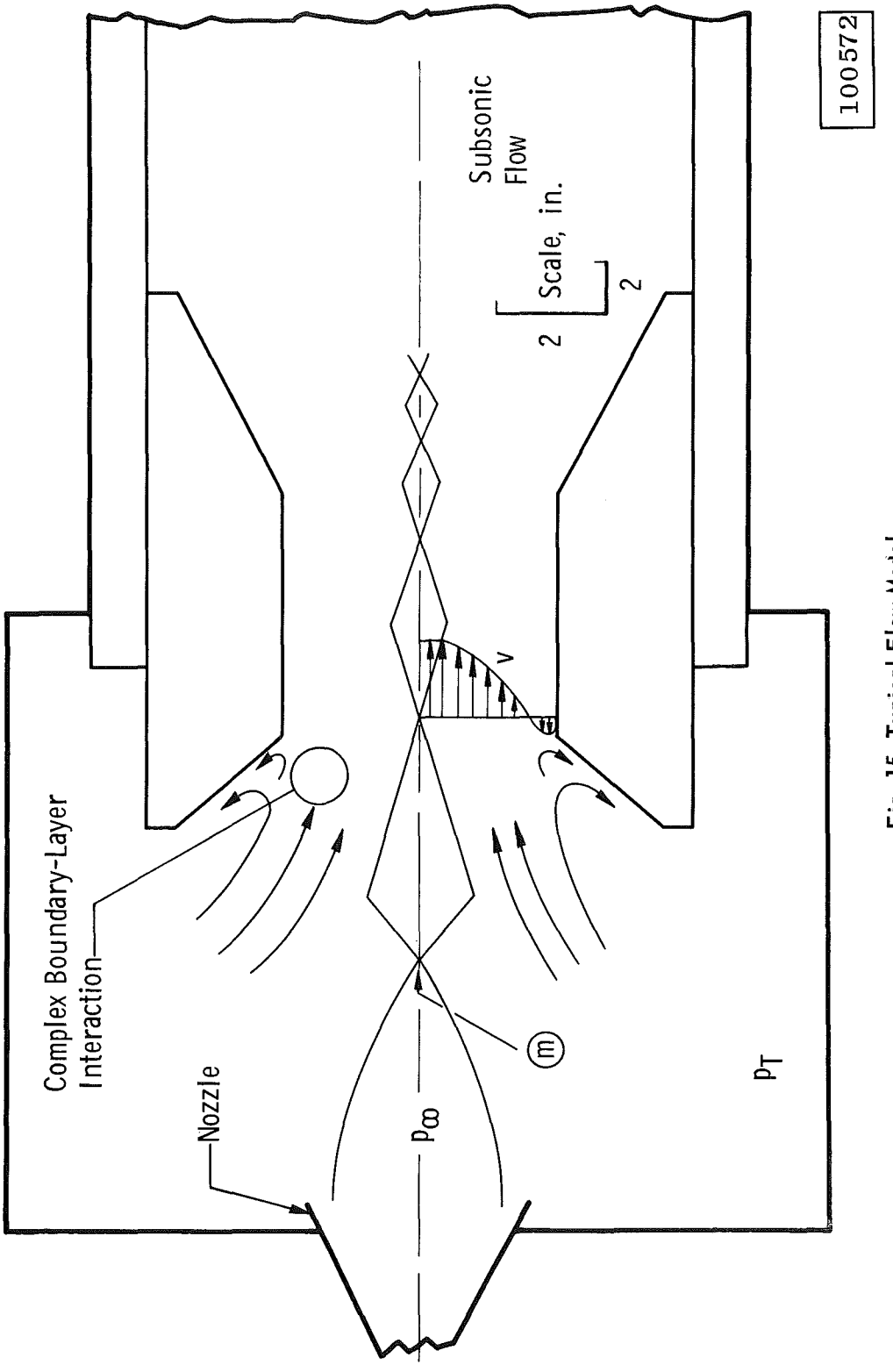

Fig. 15 Typical Flow Model

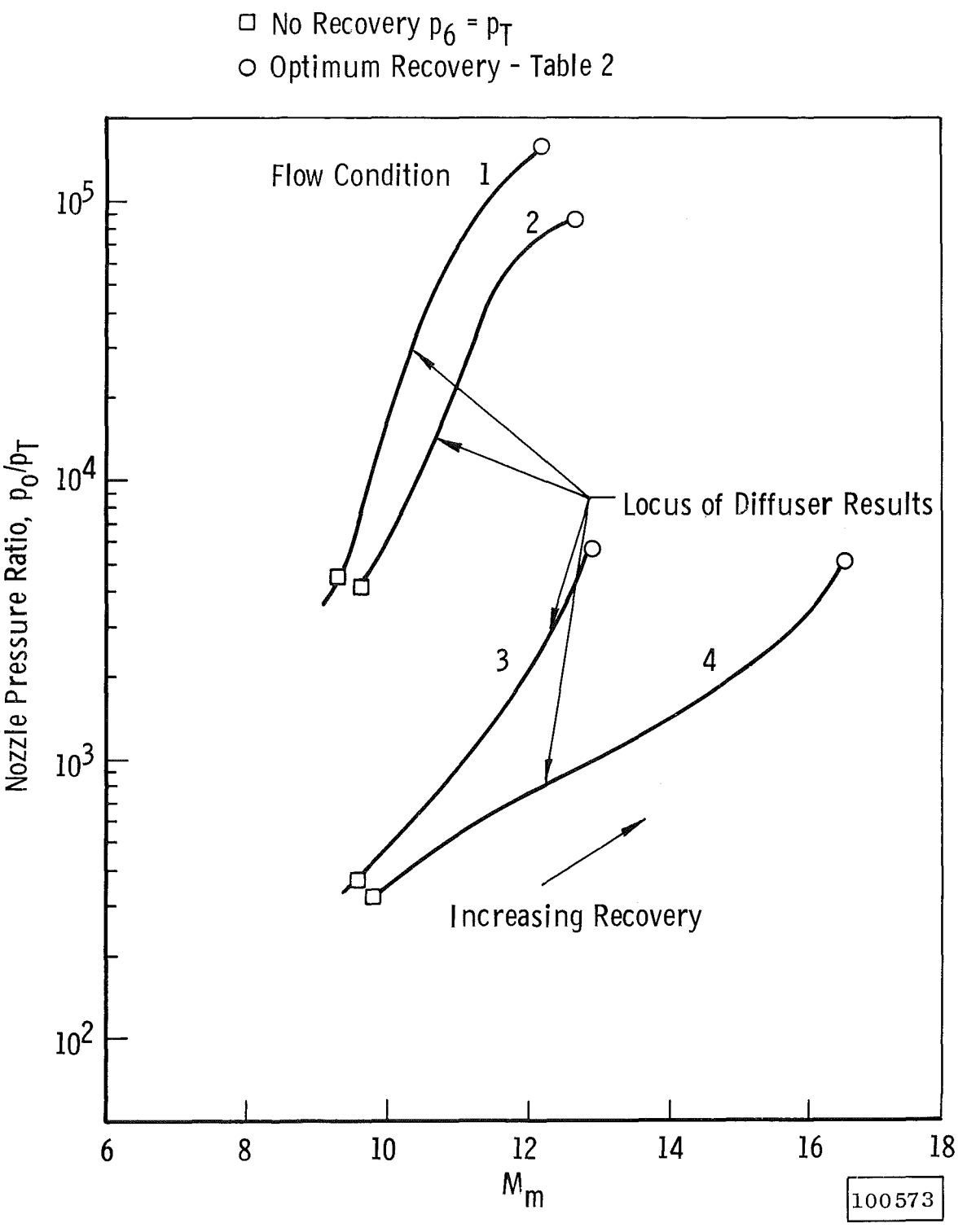

Fig. 16 Pressure Ratios Available

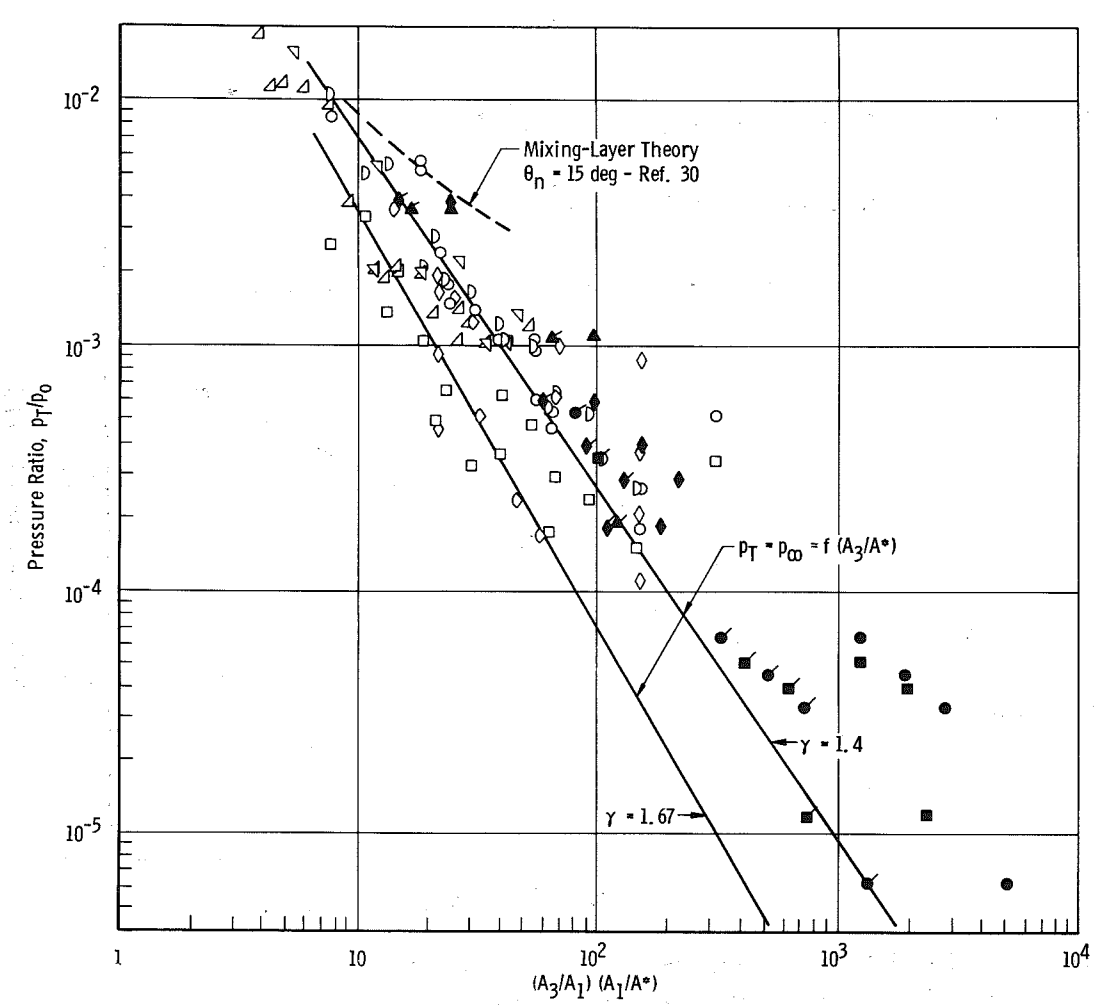

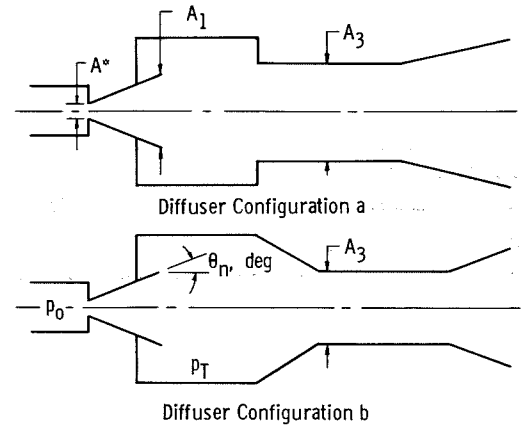

Symbol	Ref.	Diffuser	θ_n	γ	Notes
◿	21	b	18^0	1.40	Data Points
○	23	a	↕	↕	Represent
□	24	b			Lowest Values
◇	25	a			of p_T Obtained
D	26	a	18^0		with Each
◁	27	a	15^0		Throat Size
◇	28	a	15^0	1.40	
●	Tunnel L	b	$9^0 36'$	1.40	Condition 1
■	Tunnel L	b	$9^0 36'$	1.40	Condition 2
◆	Tunnel L	b	15^0	1.67	Condition 3
▲	Tunnel L	b	15^0	1.67	Condition 4

Unflagged Symbol - True Physical Areas
Flagged Symbol - A_1/A^* from One-Dimensional Area Ratio Corresponding to Calibrated M_1.
A_3/A_1 from True Physical Areas

Data with $A_3 > (A_3)_{opt}$ Omitted from Tunnel L Data

100574

Fig. 17 Effect of Diffuser Area Ratio on Test Chamber Pressure

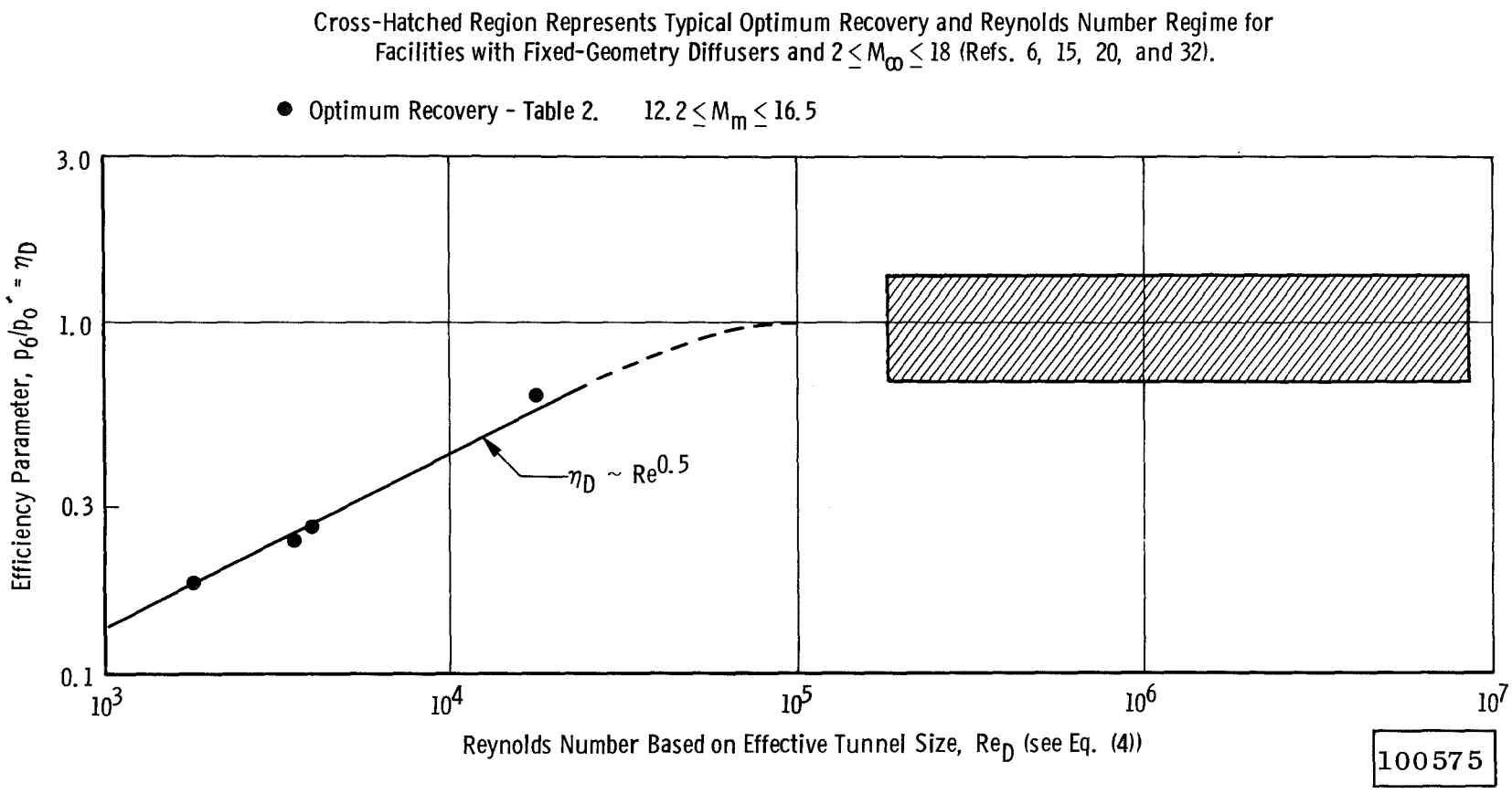

Fig. 18 Diffuser Efficiency as a Function of Reynolds Number

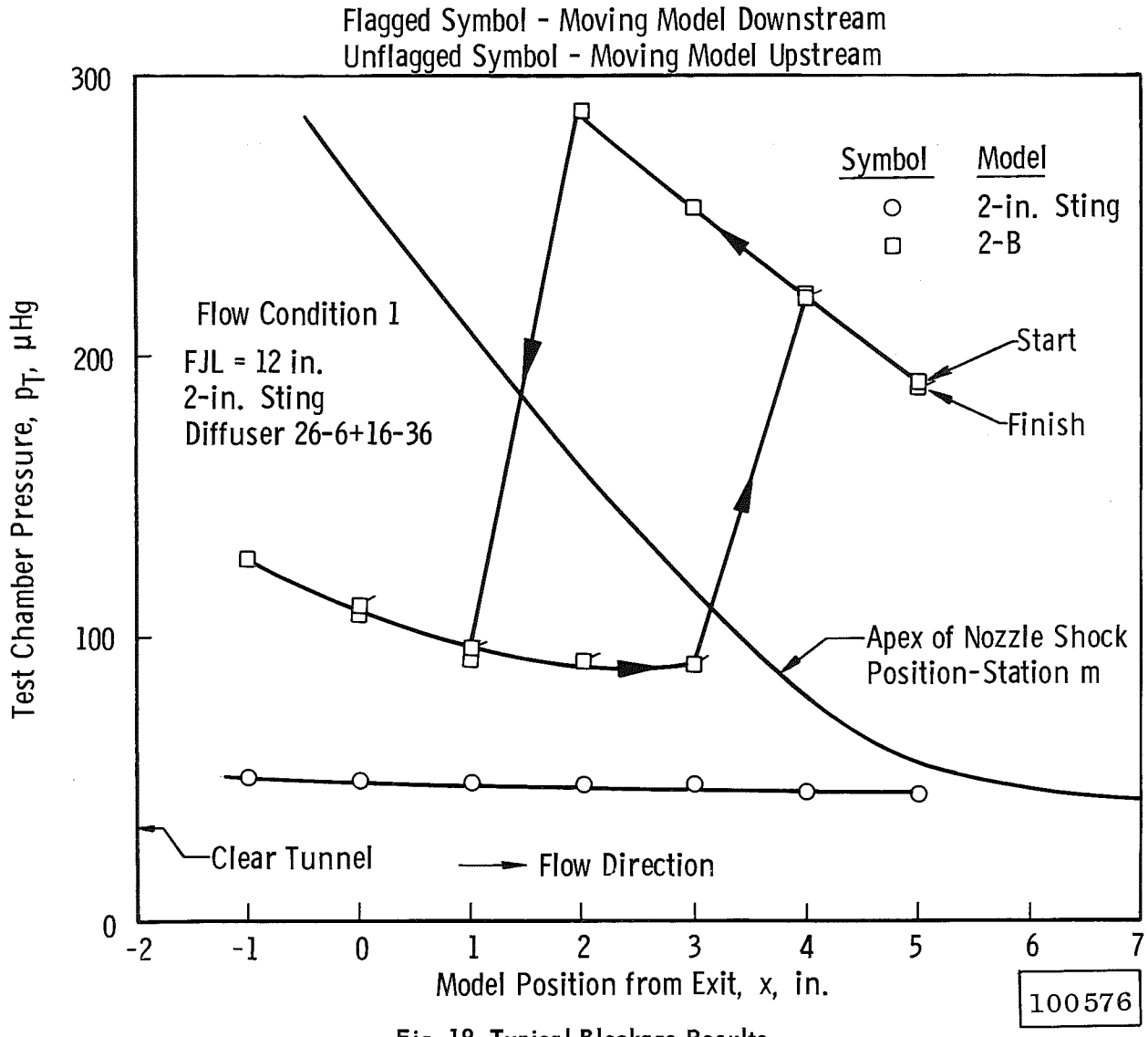

Fig. 19 Typical Blockage Results

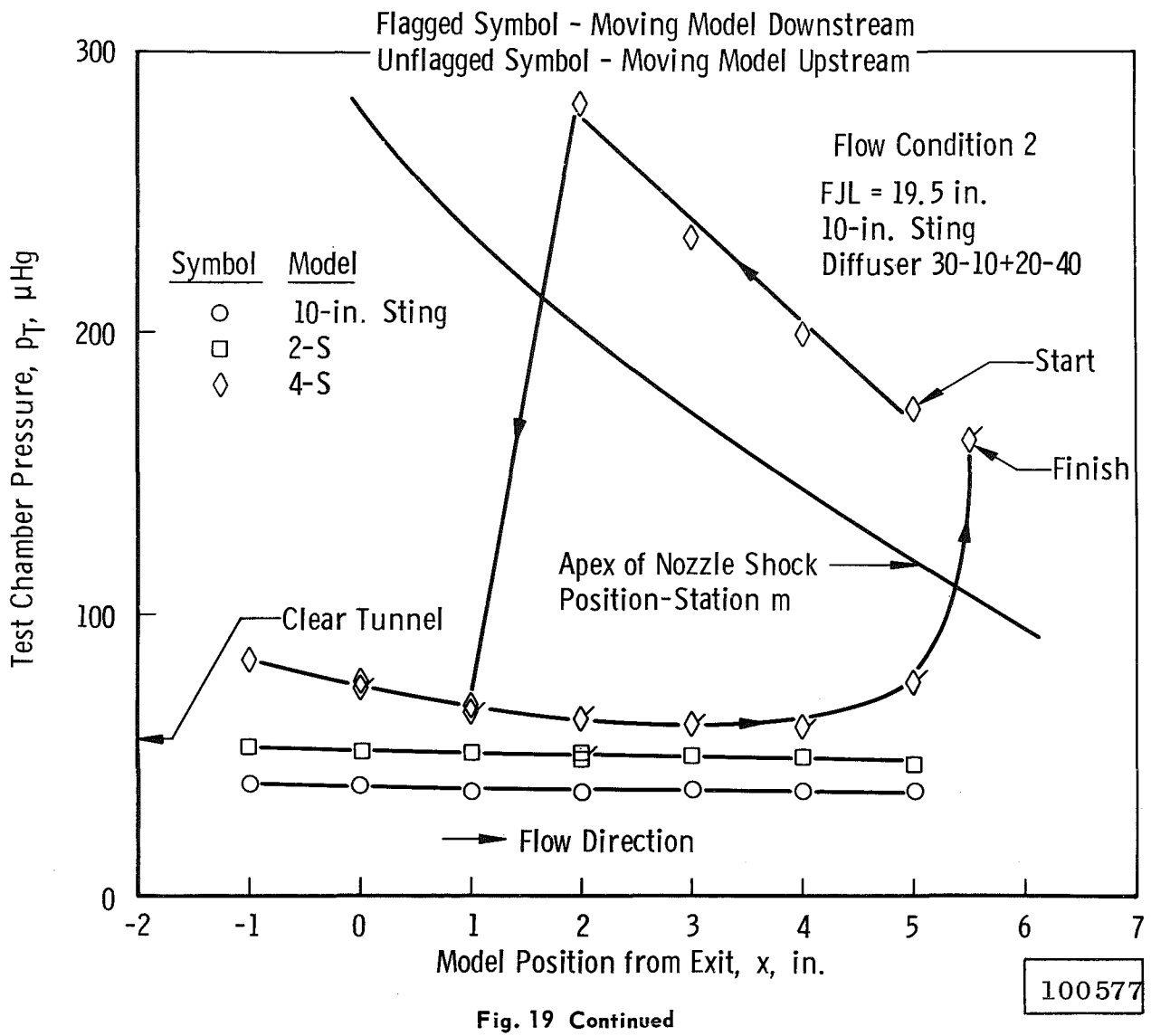

Fig. 19 Continued

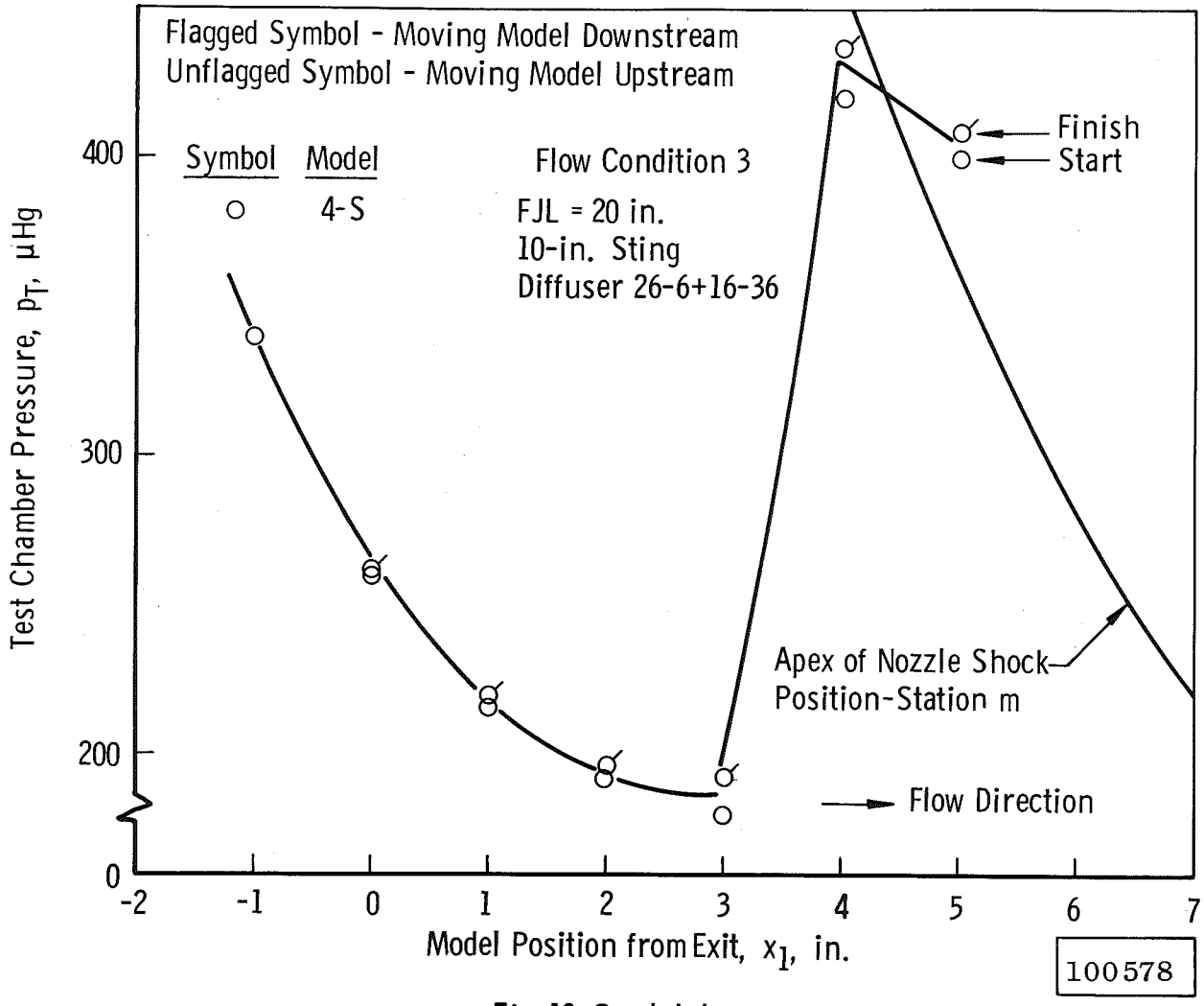

Fig. 19 Concluded

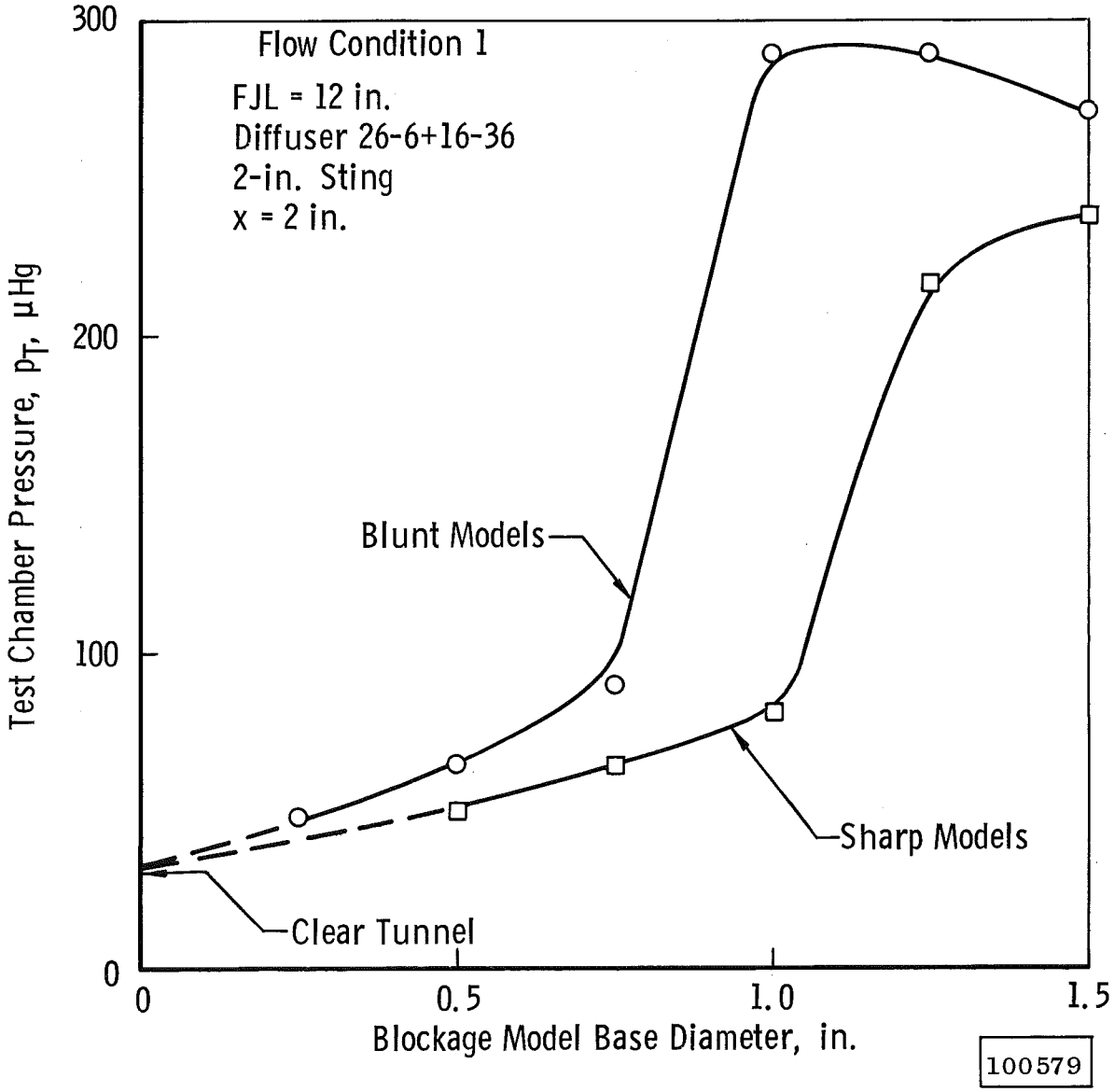

Fig. 20 Effect of Model Size and Shape on Tunnel Blockage

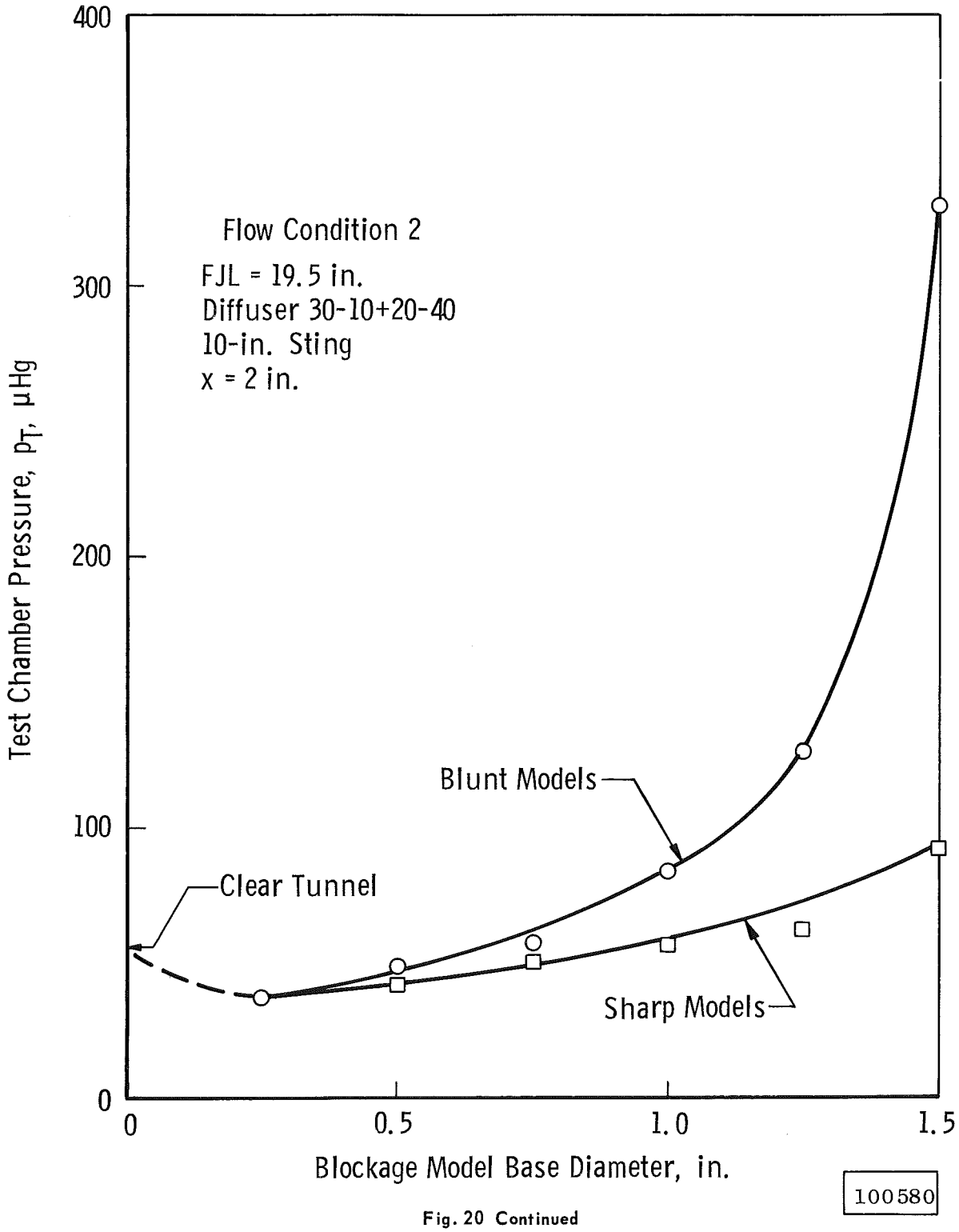

Fig. 20 Continued

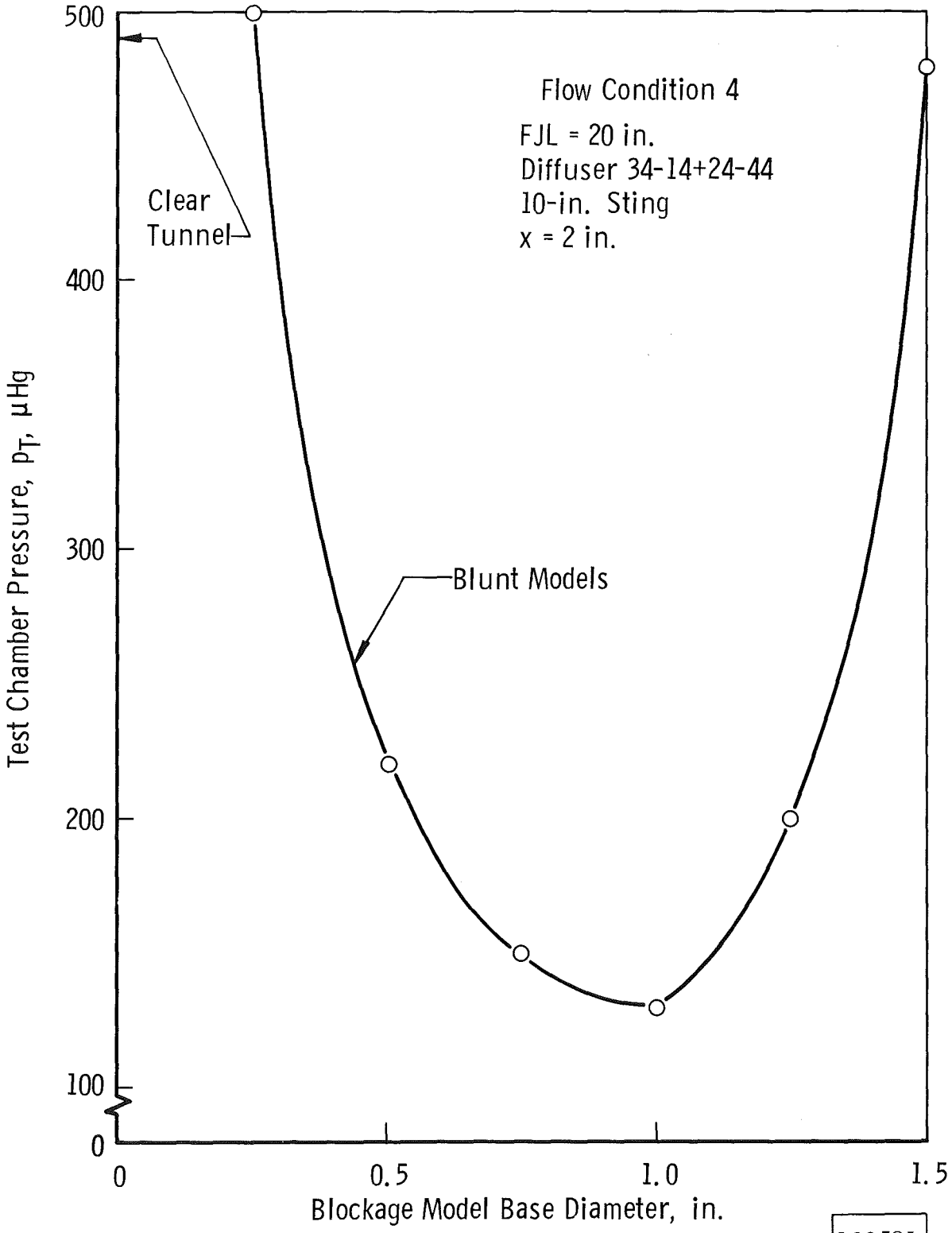

Fig. 20 Concluded

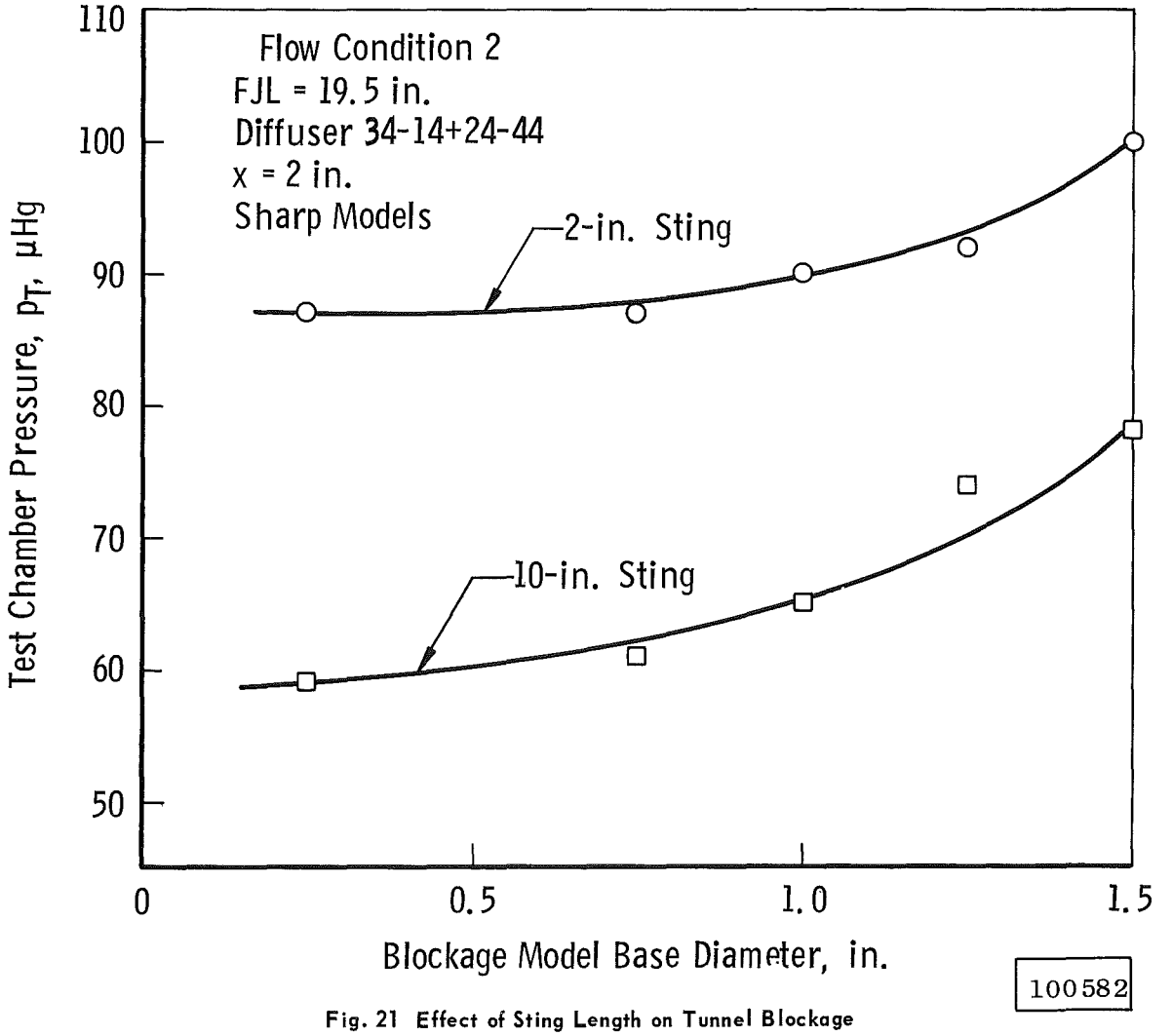

Fig. 21 Effect of Sting Length on Tunnel Blockage

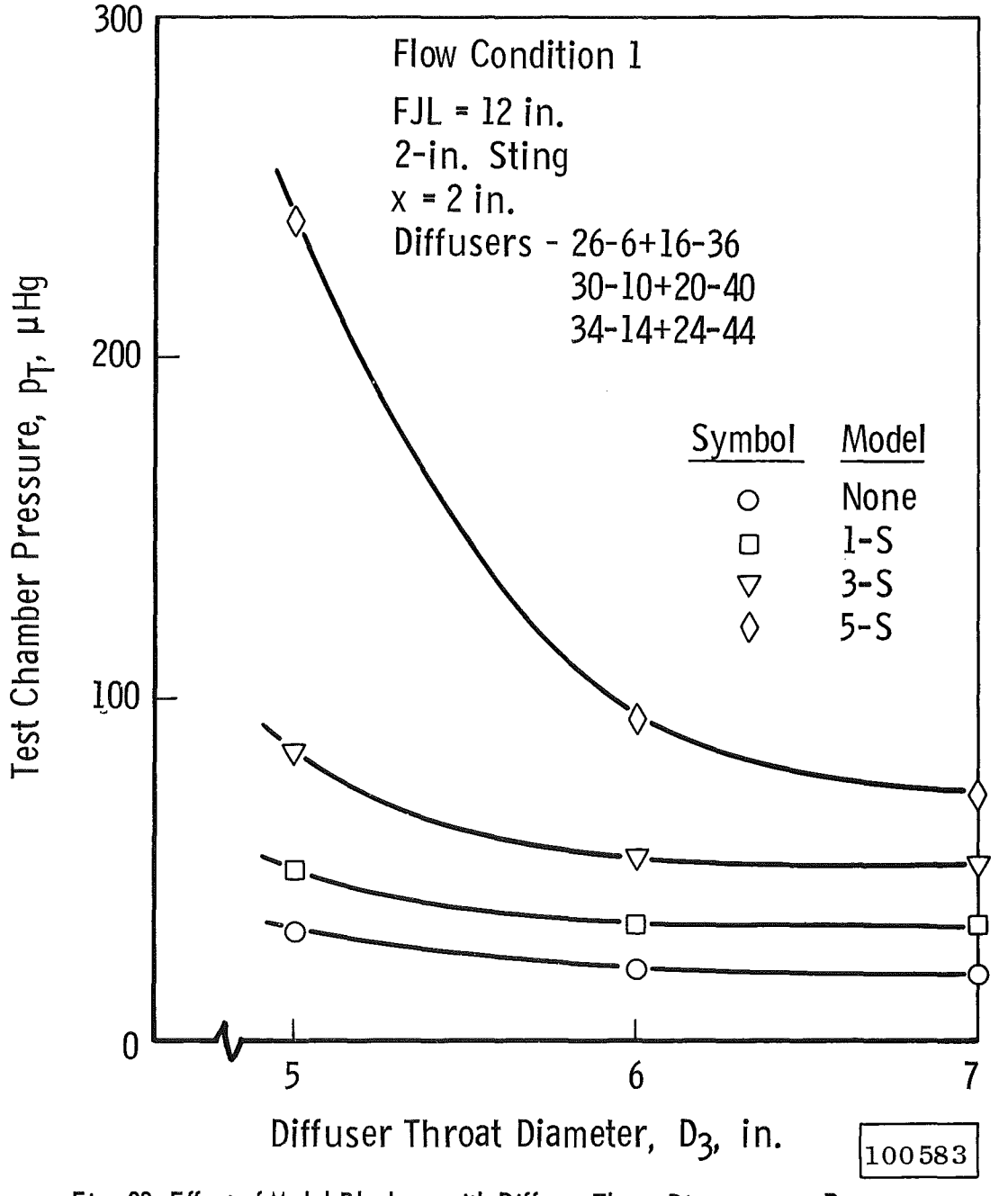

Fig. 22 Effect of Model Blockage with Diffuser Throat Diameter as a Parameter

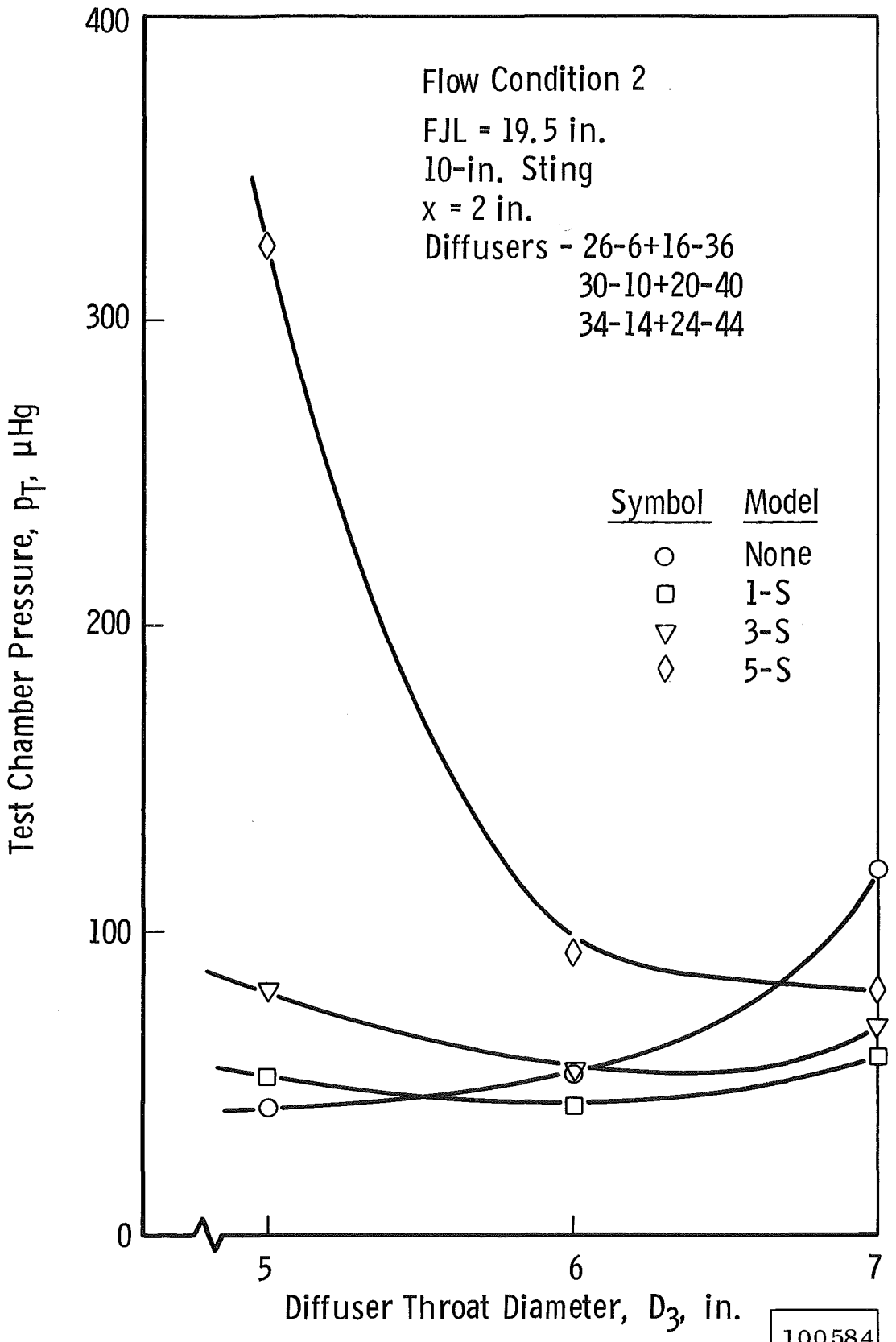

Fig. 22 Continued

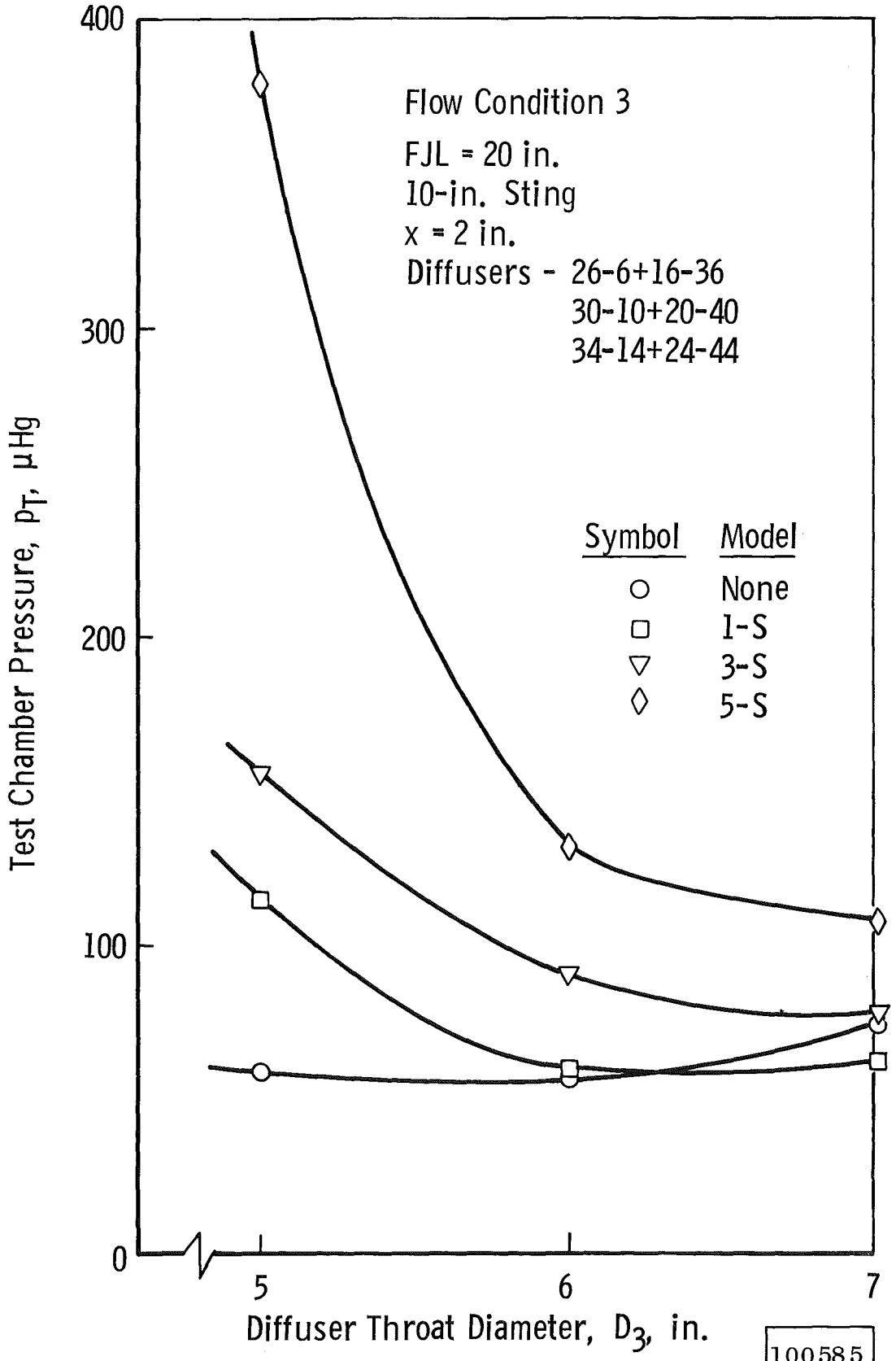

Fig. 22 Continued

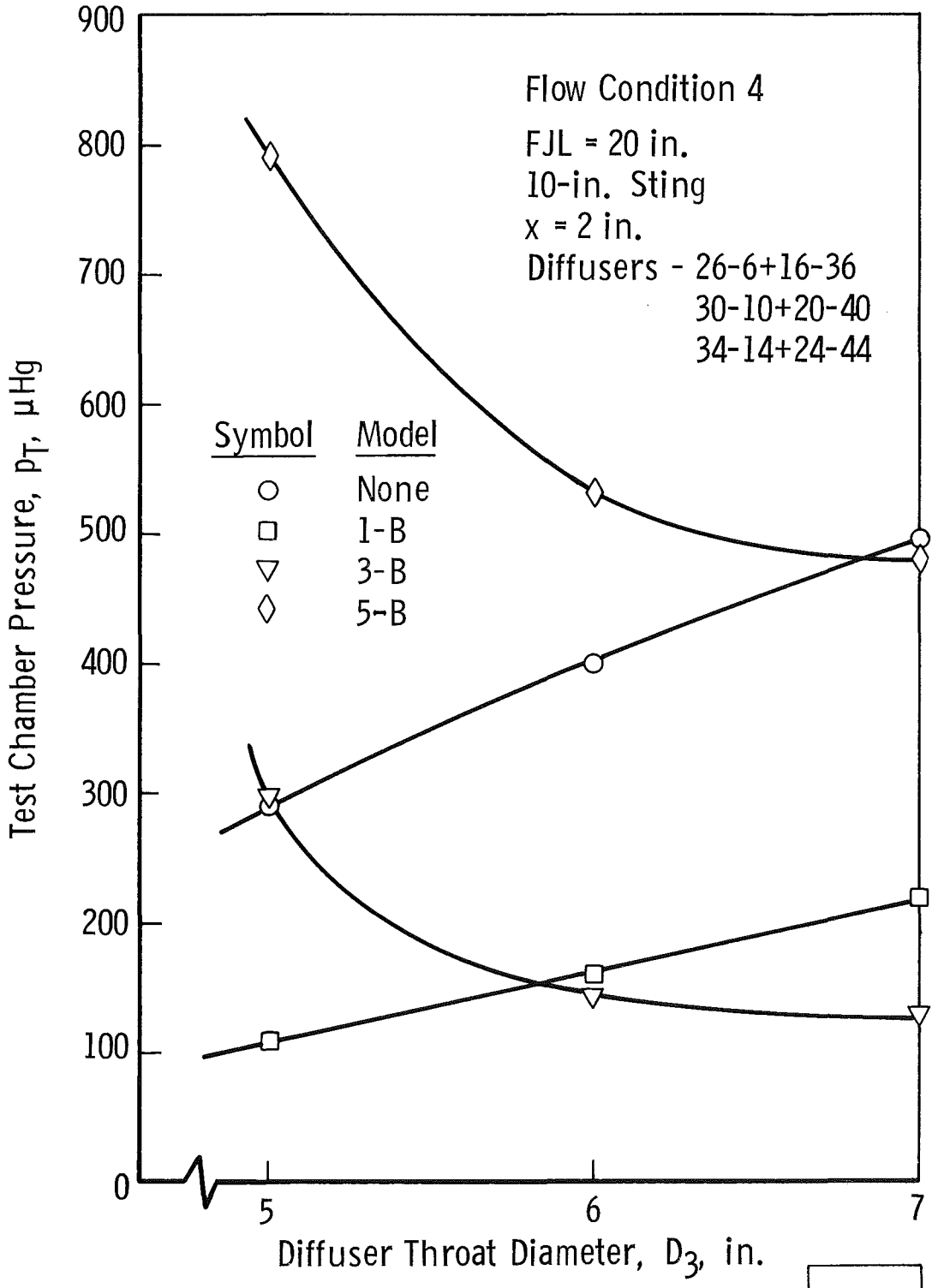

Fig. 22 Concluded